Keratinocyte Expression of CGRPβ: Implications for Neuropathic and Inflammatory Pain Mechanisms

Q Hou[1], **TP Barr**[1], **LE Gee**[1], **JT Vickers**[1], **JP Wymer**[2], **E Borsani**[3], **LF Rodella**[3], **S Getsios**[4], **TH Burdo**[6], **E Eisenberg**[7], **U Guha**[8], **RM Lavker**[4], **JA Kessler**[5], **SV Chittur**[9], **DF Fiorino**[10], **FL Rice**[1,11], and **PJ Albrecht**[1,11]

[1]Center for Neuropharmacology and Neuroscience, Albany Medical College, Albany, NY

[2]Department of Neurology, Albany Medical College, Albany, NY

[3]Division of Human Anatomy, Department of Biomedical Sciences and Biotechnologies, University of Brescia, Brescia, Italy

[4]Department of Dermatology, Northwestern University, Chicago, IL

[5]Department of Neurology, Feinberg School of Medicine, Northwestern University, Chicago, IL

[6]Department of Biology, Boston College, Chestnut Hill, MA

[7]Rambam Medical Center, and Faculty of Medicine, Israel Institute of Technology, Haifa, Israel

[8]Cancer Biology & Genetics, Slone-Kettering Institute, New York, NY

[9]Center for Functional Genomics, SUNY Albany, Rensselaer, NY

[10]In Vivo Pharmacology, Vertex Pharmaceuticals, San Diego, CA

[11]Integrated Tissue Dynamics, LLC, Rensselaer, NY

Abstract

Calcitonin Gene-Related Peptide (CGRP) is a vasodilatory peptide that has been detected at high levels in the skin, blood, and cerebral spinal fluid under a variety of inflammatory and chronic pain conditions, presumably derived from peptidergic C and Aδ innervation. Herein, CGRP immunolabeling (IL) was detected in epidermal keratinocytes at levels that were especially high and widespread in the skin of humans from locations afflicted with postherpetic neuralgia (PHN) and complex region pain syndrome type 1 (CRPS), of monkeys infected with simian immunodeficiency virus, and of rats subjected to L5/L6 spinal nerve ligation, sciatic nerve chronic constriction, and subcutaneous injection of Complete Freund's Adjuvant. Increased CGRP-IL was also detected in epidermal keratinocytes of transgenic mice with keratin-14 promoter driven overexpression of noggin, an antagonist to BMP-4 signaling. Transcriptome microarray, qPCR, and Western blot analyses using laser captured mouse epidermis from transgenics, monolayer cultures of human and mouse keratinocytes, and multilayer human keratinocyte organotypic cultures, revealed that keratinocytes express predominantly the beta isoform of CGRP. Cutaneous

Corresponding author: Dr. Phillip J. Albrecht, Assistant Professor, Center for Neuropharmacology & Neuroscience, Albany Medical College, Albany, NY 12208, phone: (518)262-5821, fax: (518)262-5799, albrecp@mail.amc.edu, philalbrecht@Intidyn.com.

Publisher's Disclaimer: This is a PDF file of an unedited manuscript that has been accepted for publication. As a service to our customers we are providing this early version of the manuscript. The manuscript will undergo copyediting, typesetting, and review of the resulting proof before it is published in its final citable form. Please note that during the production process errors may be discovered which could affect the content, and all legal disclaimers that apply to the journal pertain.

The authors declare that there are no real or percieved conflicts of interest associated with the research data presented.

peptidergic innervation has been shown to express predominantly the alpha isoform of CGRP. Keratinocytes also express the cognate CGRP receptor components, CRLR, RAMP1, and RCP, consistent with known observations that CGRP promotes several functional changes in keratinocytes, including proliferation and cytokine production. Our results indicate that keratinocyte derived CGRPβ may modulate epidermal homeostasis through autocrine/paracrine signaling and may contribute to chronic pain under pathological conditions.

Keywords

Sensory transduction; Cutaneous innervation; BMP-4; Noggin; Skin; Dermatology

Introduction

Calcitonin Gene-related Peptide (CGRP) is a well-conserved neuropeptide implicated in nociception, vasoregulation, inflammation, and epidermal homeostasis [5,9,25,34,45–46,53,73,87,91–92,99,106,109,111]. Mammals express two CGRP isoforms, CGRPα and CGRPβ, derived from separate genes, but which remain largely functionally indistinguishable [97,109,111]. CGRP-immunolabeling (IL) is observed on subsets of C and Aδ innervation (peptidergic) that terminate in different proportions in various skin compartments, especially the epidermis and perivascular [4,88,119]. Peptidergic innervation coexpresses a variety of combinations of receptors and ion channels, such as TrpV1 and ASIC3, and is implicated in several sensory functions, including neurogenic inflammation and nociception [3,19,33,61–62,68,76,85,94]. Although existing antibodies do not distinguish between the two isoforms, mRNA assessments of dorsal root ganglion neurons indicate that peptidergic cutaneous innervation predominately expresses the CGRPα isoform with only limited CGRPβ expression [71,74]. Immunochemical assays have detected the presence of CGRP in plasma, CSF and spinal cord [112], and increased levels of CGRP have been documented in the skin, blood, and cerebral spinal fluid from a variety of human and animal chronic pain conditions [5–7,13,17,20,46,51,72,103]. Therefore, CGRP has become a leading target for chronic pain therapeutics [9,32]. The increased CGRP is presumed to arise from excess release of CGRPα from sensory endings and central terminations of peptidergic fibers contributing to nociceptive pathways [9,12,35–36,52,58,90,109,116].

Like neurons, keratinocytes are derived from ectoderm and express a wide variety of neurochemical properties [81,92,96,101,117]. Whereas neurons largely remain postmitotic and terminally differentiated, keratinocytes are replaced through proliferation at the basal layer and undergo phased differentiation as they are displaced superficially and shed [38–39]. Until recently, the neurochemical properties of keratinocytes have been examined in the context of epidermal barrier homeostasis and wound repair [26–28,92,101]. In this context, CGRP has been shown to promote keratinocyte proliferation and cytokine expression, with the source of the CGRP assumed to be from peptidergic sensory endings in the epidermis [34–35,53,92,99,106]. Recent data have demonstrated that epidermal keratinocytes have a dynamic, stratified neurochemical organization that may play a direct role in sensory transduction and modulation of sensory ending function [64,88]. Moreover, pathologies of the epidermal chemistry, particularly the de novo expression of voltage-gated sodium channels, have been implicated in excessive keratinocyte-derived ATP release, likely contributing to chronic pain [33,117]. We have consistently observed low levels of CGRP-IL expressed heterogeneously among epidermal keratinocytes, with indications of increased homogeneous expression under some chronic pain conditions.

The purpose of this study was to determine whether CGRP-IL is consistently increased among epidermal keratinocytes under chronic pain conditions and whether CGRP-IL in keratinocytes is accompanied by mRNA expression for CGRPα and CGRPβ isoforms. Our results indicate that CGRP-IL is increased in painful skin sites of humans with postherpetic neuralgia and complex regional pain syndrome type1, of rats caused by L5/L6 spinal nerve ligation, sciatic nerve chronic constriction injury, and by subcutaneous administration of Complete Freund's Adjuvant (CFA), and of monkeys infected with SIV. Surprisingly, mRNA analyses indicate that the keratinocytes produce predominantly CGRPβ, which may normally play an autocrine/paracrine role in epidermal homeostasis, but may contribute to chronic pain under pathological conditions.

Methods

Animals

All animal experiments performed at each site were approved by the Institutional Animal Care and Use Committees of Albany Medical College (SNL), Northwestern University (transgenics), University of Maryland (CFA), University of Brescia (CCI), and Harvard University's New England Regional Primate Research Center (SIV), in accordance with standards of the American Association for Accreditation of Laboratory Animal Care, and conformed to the guidelines set forth by the Society for Neuroscience care and use of laboratory animals, and the ethical standards set forth by the Committee for Research and Ethical Issues of the IASP [118]. All animals were maintained in viral-free facilities on a 12 hr light/dark cycle with *ad libitum* food and water. Monkeys were housed individually (SIV), rats were housed individually (SNL, CCI, RMI) or 2–3 per cage (CFA) and transgenic mice were housed 4–6/cage.

Humans

Tissue obtained from human subjects (CRPS, PHN) was done utilizing protocols for study design approved by the local Institutional Review Board (IRB) of the Rambam Medical Center Ethic Committee (CRPS) and Albany Medical College (PHN, DN).

Human Pain Conditions

Post-herpetic Neuralgia—Five subjects with PHN and six controls subjects were recruited whose demographics are summarized in Table 1. A concerted attempt was made to match the ages, genders, and biopsy sites of the PHN and control subjects. Subjects were rated "yes" or "no" for hypertension (HTN), elevated cholesterol (Chol) and hypothyroidism (hypothyr). In all the figures, the data are labeled by the age and gender (e.g. 66F = 66 year-old female). For control subjects, a single punch biopsy (3mm) was taken from symmetrical left and right locations. For the PHN subjects, one biopsy was taken from the most painful site that had been afflicted by a rash (ACTIVE), another site 1 cm apart (IPSI) and a mirror image location in the contralateral dermatome (CONTRA). One PHN subject was substantially younger (29 years old) than the four other PHN subjects and had a substantially higher VAS score. He was only 22 years old at the time of his acute zoster attack and the persistence and severity of his chronic pain was unusual for his age. He was grossly overweight >350 pounds. For comparison, a 23 year old male control subject of comparable weight was recruited.

Complex Regional Pain Syndrome (CRPS): Human CRPS type I tissue was obtained from the surgically amputated upper limb (arm) and lower limb (leg) of separate patients. Full patient clinical descriptions, tissue handling, and certain pathologic alterations of this tissue have been published previously [3]. Changes of epidermal chemistry had been noted

by the authors at the time of that publication (personal communication), but were too undefined to include as part of that work.

Diabetic Peripheral Neuropathy: Five diabetic and five nondiabetic subjects were recruited whose demographics are summarized in Supplementary Table 1. A concerted attempt was made to match the ages and genders of the diabetic and nondiabetic subjects. Subjects were rated "yes" or "no" for hypertension (HTN), elevated cholesterol (Chol) and hypothyroidism (hypothyr). A single punch biopsy (3mm) was taken from the glabrous lateral edge of the non-dominant foot from each subject about halfway between the base of the 5th digit and the end of the heel. All 5 subjects had diagnosed diabetic peripheral neuropathy (DPN) with chronic pain >2.0 VAS. In addition to the PHN patient data, Supplementary Table 1 includes peroneal and sural nerve conduction velocities (PerCV and SuralCV in meters/second) and sural nerve amplitudes.

Nerve injury

Spinal Nerve Ligation (SNL)—To determine the potential impact of nerve injury on CGRP expression in epidermal keratinocytes, a unilateral tight spinal nerve ligation (SNL) of the L5 and L6 spinal nerves was performed under isofluorane anesthesia on male Sprague-Dawley rats (150–200 gr., Taconic Farms, Germantown, NY) following the methods of Kim and Chung [59], with slight modifications (Fig. 1A). Briefly, a midline incision was made over the lumbar vertebral ridge, and back musculature opened to reveal the L6 transverse process. The process was removed and the L4, L5, and L6 spinal nerves were exposed using a pulled glass pipet. The L5 and L6 spinal nerves were tightly ligated, while the L4 nerve root was gently irritated by light rubbing and stretching. Animals were closed and allowed to recover for 5–7 days. Neuropathic pain was monitored by measures of mechanical allodynia using nylon fibers of differing thickness to impart mechanical deflection of the rat hindpaw plantar surface (Von Frey filaments). Baseline testing was performed prior to surgeries, and again on days 3–4, 10, 30, and 60 days post SNL. Results were compared by repeated measures ANOVA with Tukey's post test. A total of 12 animals were utilized (3 remained as control for the full 60 days, 3 underwent sham surgeries and were tested out to 60 days, and 6 underwent SNL procedures). Sham surgeries involved all but the nerve ligations and L4 manipulation. The 30 day SNL animals (n=3), and all remaining animals following 60 day testing, were sacrificed by transcardial perfusion with 4% paraformaldehyde and the ipsilateral and contralateral hindpaws bluntly removed, post-fixed for 4 hr in 4% PFA, transferred to fresh PBS with 0.1% NaN_3 and stored at 4°C for subsequent immunofluorescence evaluation.

Sciatic nerve loose ligature (CCI)—Loose ligature chronic constriction injury (CCI) was also used as another animal model of chronic neuropathic pain. Ten Sprague-Dawley rats were anesthetized by intraperitoneal injection of Zoletil (60 mg/kg; Virbac, France), and the right sciatic nerve was exposed at the level of the mid-thigh by blunt dissection and separated from the adhering tissue immediately proximal to its trifurcation. In 5 rats, four ligatures were then loosely tied around the nerve at 1–2 mm distance using 4–0 chromic gut suture material (Fig. 1A) [10]. The other 5 rats were sham-operated controls where the left sciatic nerve was exposed at the same level, without ligature. Responses to thermal stimuli of all animals were measured before and 3, 7, and 14 days after the CCI or sham surgical procedure. Measurements were performed on both the ipsilateral and contralateral hind paws of all rats by researchers who were blind to treatments. Thermal hyperalgesia was tested according to the Hargreaves procedure [49] using a plantar test apparatus (Ugo Basile, Comerio, Italy). Briefly, rats were placed in clear plexiglass cubicles and allowed to acclimatize. A constant intensity radiant heat source (beam diameter 0.5 cm and intensity 40 I.R.) was aimed at the midplantar area of the hind paw. The average withdrawal latency

time, in seconds (s), from initial heat source activation until paw withdrawal was determined in four separate trials for each time point. Results were compared by repeated measures ANOVA with Tukey's post test. Animals were sacrificed at 14 days by transcardial perfusion with 4% paraformaldehyde and the ipsilateral and contralateral hindpaws bluntly removed, post-fixed for 4 hr in 4% PFA, transferred to fresh PBS with 0.1% NaN_3 and stored at 4°C for subsequent immunofluorescence evaluation.

Inflammation Injury

Complete Freund's Adjuvant (CFA)—To test directly the potential impact of tissue inflammation on CGRP expression in epidermal keratinocytes, male Sprague-Dawley rats (150–300 gr, Harlan, Indianapolis) were administered Complete Freund's Adjuvant (CFA, Sigma, St. Louis) suspended in an oil/saline (1:1) emulsion and injected (0.1 mg *mycobacterium* sc) into a plantar hindpaw. The injection produces an intense tissue inflammation characterized by erythema, edema, and hyperalgesia [8,23]. Control animals (n=2), and plantar hindpaw vehicle-injected animals (n=2) were maintained for 14 days without signs of discomfort or stress. Nine CFA injected animals (n=3/group) were utilized for hindpaw immunochemistry evaluation at 2 hr, 3 day, and 14 day following CFA injection. All animals were sacrificed by transcardial perfusion with 4% paraformaldehyde (PFA) and the ipsilateral (injected) and contralateral hindpaws bluntly removed, post-fixed for 4 hr in 4% PFA, transferred to fresh PBS with 0.1% NaN_3 and stored at 4°C for subsequent immunofluorescence evaluation.

Viral infection (SIV)—To investigate potential keratinocyte alterations associated with viral-induced inflammation, skin samples were taken from monkeys utilized for modeling simian immunodeficiency virus (SIV) encephalitis (Table 2). Rhesus monkeys were infected with SIVmac251 (20 ng of SIV p27) by intravenous injection, provided by Ronald Desrosiers (Harvard University's New England Regional Primate Research Center). To achieve rapid progression to AIDS with a high incidence of SIV encephalitis, monkeys were CD8+ T-lymphocyte depleted, via treatment with a human anti-CD8 antibody, cM-T807, administered s.c. (10mg/kg) at day 6, as well as i.v. (5mg/kg) at days 8 and 12 following infection [18,95,110]. Antibodies were provided by the NIH Non-human Primate Reagent Resource (RR016001, AI040101). CD8+ T-lymphocyte depletion was monitored by flow cytometry prior to antibody treatment and weekly during the infection. Upon the development and progression of AIDS, 4 animals were sacrificed by anesthetization with ketamine-HCl, euthanized by an intravenous pentobarbital overdose and exsanguinated. For these studies, glabrous palmar and plantar skin samples were removed, immersion-fixed for 4 hr in 4% PFA, transferred to fresh PBS with 0.1% NaN_3 and stored at 4°C for subsequent immunofluorescence evaluation. Control hypothenar skin samples were collected from a normal, uninfected control animal, under general anesthetic, and identically processed. Skin samples from other normal monkeys had been previously processed as part of prior studies [77–79].

TGFβ Regulation

Transgenic mice—It has been previously shown that BMP family members, including BMP-4, can induce CGRP expression in cultured neurons [1]. As well, our own studies have demonstrated that CGRP-expressing DRG neurons and peptidergic CGRP skin innervation were also impacted by relative amounts of BMP-4 and noggin over-expression in the epidermis of transgenic mice [48]. Interestingly, during those studies, preliminary assessments indicated that noggin anatagonism of BMP4 signaling appeared to increase CGRP-IL in the epidermis. To confirm CGRP-IL expression in keratinocytes and to test whether immunofluoresent intensity reflects CGRP expression, BMP4- and Noggin-overexpressing transgenic mice were used for CGRP mRNA evaluations of epidermal

keratinocytes. BMP4- and Noggin-overexpressing transgenic mice were generated in the laboratory of Dr. John Kessler [48]. Mouse Noggin cDNA was PCR amplified from E19 whole brain RNA, and the sequence was verified and subcloned into p-Bluescript (pBKS-Noggin). The noggin fragment was then subcloned into the K14-hGH poly(A) plasmid [23] to make the K14-Noggin-hGH poly(A) plasmid, which contains the keratin-14 promoter and the human growth hormone exon/intron and poly(A) sequences. The vector was digested, and the K14-Noggin-poly(A) fragment was injected into one-cell FVB embryos to generate Noggin-overexpressing mice. The BMP4 cDNA, also amplified from mouse RNA, was similarly subcloned into the K14-hGH poly(A) plasmid and injected into CB6F1 one-cell embryos to generate the BMP4-overexpression mice. The transgenic founders were identified by Southern blot analysis, and further screening was performed by PCR with transgene-specific primer pairs. Adult mice (6–8 wks) over-expressing noggin or BMP-4 (n=6/group) were sacrificed by transcardial perfusion with 4% paraformaldehyde (PFA) and the hindpaws bluntly removed, post-fixed for 4 hr in 4% PFA, transferred to fresh PBS with 0.1% NaN_3 and stored at 4°C for subsequent immunofluorescence evaluation. For laser capture microdissection (LCM) and subsequent transcriptome array analyses and qPCR, adult (6–8 wks) noggin and BMP4 transgenic mice (n=6/group) were killed by lethal ketamine ip injection, hindpaws were rapidly removed, glabrous skin dissected free and placed corium-side down onto a small sponge to retain a flat tissue shape, and snap frozen in liquid N_2. Tissue blocks were maintained at −80°C until subsequent processing for LCM/qPCR.

Tissue Processing—Immersion and perfusion fixed glabrous tissue specimen (mouse, rat, monkey, human) were cryoprotected by overnight infiltration with 30% sucrose/PBS, embedded in Optimal Cutting Temperature (OCT) mounting media, snap frozen, and cut by cryostat into 14 µm sections perpendicular to the skin surface and parallel to the long axis of the sample. Sections were rotated across a series of at least 10 slides to allow immunolabeling of alternating sections with various combinations of antibodies against different target antigens. The sections were thaw mounted onto chrome-alum-gelatin-coated slides, air-dried overnight, and processed for single or double immunolabeling. Flash-frozen tissue for LCM/qPCR were similarly cut, but utilized standard precautions to prevent contamination from RNAses, including complete cleaning of the cutting knife and all surfaces of the cryostat with an RNAse eliminating detergent (RNaseZap). Sections were quickly thaw-mounted onto RNAse-free superfrost plus glass slides, ~5/slide, well-spaced to allow for laser etching, and maintained at −20°C until LCM.

Cultured epidermal keratinocytes

Human keratinocytes—Primary human epidermal keratinocytes from neonatal foreskin (Lonza, Basel) were cultured with chemically defined keratinocyte growth media (KGM-CD, Lonza) supplemented with 0.5% penicillin/streptomycin antibiotics and maintained at 37°C and 5% CO_2. Primary human epidermal keratinocytes were plated on collagen coated 35mm dishes at a density of 3,500–10,500 cells/cm^2 and grown until 95–100% confluent, with media refreshed every 48–72 hrs. Total RNA was extracted from confluent keratinocyte cultures that were maintained in basal, low calcium KGM, or from those that were switched into high calcium media (2mM $CaCl_2$) for 5 additional days to increase differentiation in these submerged cultures, as previously described [50,115]. To fully differentiate keratinocytes *in vitro*, normal human epidermal keratinocytes were grown at an air-liquid interface for 12 days to generate organotypic raft cultures of human epidermis [43]. Mature raft cultures were then processed for total mRNA and protein recovery and subjected to qPCR and Western blot analysis, respectively.

Mouse Keratinocytes—Isolation of epidermal keratinocytes from neonatal mice was based on a published protocol [31]. The epidermis from a newborn mouse yields approximately $5–10×10^6$ cells. Cells are cultured in calcium-free Eagle's minimal essential medium (EMEM), supplemented with 4% fetal bovine serum (FBS), 0.05mM $CaCl_2$, 0.4ug/ml hydrocortisone, 5ug/ml insulin, 10ng/ml epidermal growth factor (EGF), $2×10^{-9}$ M T3, 100 units/ml penicillin and 100ug/ml streptomycin, 2mM L-glutamine, and cholera toxin (10^{-10}M). Cells were kept at 33°C, 8% CO_2 for five to seven days before use in experiments. In addition, a mouse keratinocyte cell line (MK-116) was derived from wild-type mouse keratinocytes, and conditionally immortalized with SV40 large T antigen [30]. MK116 cells were cultured in the identical media as primary mouse cultures, with the exception of the cholera toxin, and the inclusion of 10 units/ml interferon-γ. MK116 cells were kept at 33°C incubator with 8% CO_2, and routinely split (1:5) when confluent to maintain culture integrity.

Analytical Techniques

Immunofluorescence—Slides were processed for single or double label immunofluorescence following published procedures [3,40,77]. Slides were preincubated in 1% bovine serum albumin and 0.3% Triton X-100 in PBS (PBS-TB) for 30 min and then incubated with primary antibody diluted in PBS-TB overnight in a humid atmosphere at 4°C. Slides were then rinsed in excess PBS for 30 minutes and incubated for 2 hr at room temperature with the appropriate Cy3-, or Alexa488-conjugated secondary antibodies (Jackson ImmunoResearch, West Grove, PA; Molecular Probes, Eugene, OR) diluted in PBS-TB (1:500). Following secondary antibody incubation, the sections were rinsed for 30 min in PBS and were either coverslipped under 90% glycerol in PBS or processed for a second run of primary and secondary antibodies before being coverslipped. The primary antibodies used are shown in Table 3. As shown in prior studies [3,41,77], anti-PGP labels all known types of peripheral innervation, anti-200kD neurofilament protein (NF) labels Aβ and likely Aδ fibers in normal mature skin, and anti-CGRP labels peptidergic subsets of C fibers (NF-negative) and Aδ fibers (NF-positive).

For rat studies where control and experimental tissues were received at the same time, control and experimental sections were immunolabeled at the same time. For the human PHN studies, control and pain site biopsies from the same patient were processed at the same time, but biopsies from different patients were received at widely different times and were processed as they were received. For the patient with CRPS afflicting the leg, biopsies from painful and nonpainful sites were received and processed at the same time. For the patient with CRPS afflicting the arm, control specimens came from normal other subjects and were processed the same way, albeit at different times but with the same lots of antibodies. Likewise, monkey specimens and specimens for the human DPN study were received and processed similarly at widely different times and, consequently, with two different lots of CGRP antibody from the same supplier.

Image Analysis—Immunostained sections were analyzed with an Olympus Optical Provis AX70 microscope equipped with conventional fluorescence filters (Cy3: 528–553 nm excitation, 590–650 nm emission; Cy2/Alexa488: 460–500 nm excitation, 510–560 nm emission). Fluorescent images were collected with a high-resolution camera (Sony, DKC-ST5) interfaced with Northern Eclipse (Empix Imaging, Mississaugau, ON), Photoshop (Adobe, San Jose, CA), and NeuroLucida (MicroBrightField, Colchester, VT) software. Camera settings were kept identical between image captures to demonstrate differences in immunolabeling intensities. For experiments assessing the relative immunofluorescent labeling as a measure of expression levels of CGRP (CGRP-IL) within epidermal keratinocytes (PHN, CRPS, SNL, CFA, SIV, DN), slides of tissue sections were blinded and

relative levels of immunofluorescence in the epidermis across all the sections on each slide were qualitatively rated by experienced investigators (QH, PJA, FLR). Photomicrographs presented are representative of the tissue staining patterns most commonly observed across all sections from any given specimen.

Laser capture microdissection (LCM)—LCM was performed on flash-frozen sections using the Veritas machine (Arcturus Biosciences, Mountain View, CA). The sections were stained by brief immersion in hematoxylin and eosin, followed by brief dehydration in ethanol and xylene, loaded into the machine and quickly used to map the epidermis prior to performing LCM. For each sample, LCM was performed on 8 to 10 skin sections and isolated the whole epidermis from each section. The captured pieces of epidermis from the same specimen were pooled in order to generate enough RNA for study.

RNA isolation, cDNA synthesis, Transcriptome Array and real time PCR—Total RNA was isolated using the PicoPure RNA Isolation Kit (Arcturus Biosciences) from LCM samples, and by Trizol (Invitrogen) from primary mouse, NHEK, calcium differentiated NHEK, and human epidermal keratinocytes grown in organotypic raft cultures. The amount of RNA isolated was on the order of 2 to 500 ng per sample. Total RNA from three biological replicates was pooled and used as template for cDNA amplification using the NuGEN pico amplification protocol and subsequently hybridized to Affymetrix Mouse Gene ST 1.0 microarrays as per manufacturer (Center for Functional Genomics, SUNY Albany). The raw data was quantile normalized using RMA, following which probe sets that had signals in the bottom 20th percentile in all samples were excluded from further analysis. This list of filtered transcripts was then subjected to a 1.5-fold filter to select those that showed differential expression between the two conditions (noggin overexpression vs BMP4 overexpression). These results were then subjected to Student's T-test to identify genes with significant difference (P<0.5). Complementary DNA was synthesized by reverse transcription (RT) of total isolated RNA (Superscript First Strand Synthesis, Invitrogen, Carlsbad, CA). Real time PCR reactions were conducted in triplicates using the following protocol: a single 3 minute step at 95°C followed by 40 cycles of 10 seconds at 95°C, 10 seconds at 55°C, and 30 seconds at 72°C. A Biorad CFX96 qPCR system was used with a C1000 thermocycler and data was analyzed with CFX Manager V1.5. Target gene expression was normalized to the housekeeping gene GAPDH. The primers were bought from Qiagen. Data from real time PCR were analyzed with student t test or ANOVA followed by Dunnett's post hoc comparisons. p<0.05 was defined as significant.

Western Blot—Cultured primary mouse keratinocytes and fibroblasts, immortalized mouse keratinocytes (MK116), and freshly isolated mouse trigeminal ganglia from adult Swiss Webster mice were lysed (RIPA cell lysis buffer) and pelleted at 12000g for 15min. Total protein from primary mouse keratinocytes (20, 40, or 60µg) and 1 or 10µg commercially available synthesized human CGRPα (used as positive control, Santa Cruz Biotechnology) were loaded and separated by 10–20% Tris/Tricine gel, and the resolved proteins were electrotransferred to 2% Nitrocellulose membrane. The membrane was then incubated with 5% non-fat milk in Tris buffer containing Tween 20 (TBS+T) for 1h and then incubated in a rabbit polyclonal anti CGRP (1:2000, Chemicon) at 4°C overnight. The membrane was subsequently washed twice with TBS+T and probed with a donkey anti-rabbit IgG conjugated with horseradish peroxidase (HRP, 1:10,000) for 1h. The membrane was then washed several times with TBS+T and visualized using and ECL chemiluminescent detection kit (Santa Cruz Biotechnology). To determine if the protein labeling was authentic, we utilized total protein from primary mouse fibroblast cultures (FB) as a negative control, immortalized and undifferentiated mouse keratinocyte monolayer cultures (MK116), and freshly dissociated and homogenized mouse trigeminal ganglia tissue

(TG) as a positive control. To determine if CGRP protein was detectable in human keratinocyte cultures, total protein samples from organotypic human keratinocytes (3D raft cultures) were loaded (5 identical 20 µg/lane samples pooled from 3 independent raft cultures), along with a CGRPα positive control lane, and subjected to identical Western procedures, except that 4–12% Bis/Tris gels were used. Additionally, to test the specificity of the anti-CGRP polyclonal antibody used to probe each Western membrane, CGRPα (1µg) and total protein samples from mouse trigeminal ganglia (TG, positive control) and mouse fibroblasts (FB, negative control) were loaded (20 µg/lane), in duplicate, subjected to Western, and the membrane then separated. One half of the membrane (left) was probed with anti-CGRP (Rb polyclonal, 1:2000; Chemicon Inc, Temecula, CA), while the other half (right) was probed with the same anti-CGRP antibody mix, but which was pre-adsorbed by incubation with excess CGRPα (1µg) and CGRPβ (1µg) for 30 min at RT. The mix was centrifuged and the resultant supernatant used for membrane probing.

CGRP Release Assays—Commercially available CGRP enzyme immunoassay kits (Cayman Chemical, Ann Arbor, MI) were used as per the manufacturer's instructions to assess whether thermal stimulation of mouse and human keratinocytes in monolayer cultures released CGRP (supplementary data).

Results

Human pain conditions (PHN, CRPS), and direct nerve injury and inflammation animal models, result in increased keratinocyte CGRP immunofluorescent labeling (CGRP-IL)

Human pain conditions: Post-Herpetic Neuralgia (PHN), Complex Regional Pain Syndrome type I (CRPS I), and Diabetic Peripheral Neuropathy (DN)—In CRPS subjects, an increase in CGRP levels has been observed in the blood and CSF, attributed to neurogenic origins [13]. Following up on observations that were not explicitly noted in some of our previous publications (e.g., Fig. 3K, Petersen et al., 2002), our current evaluations of human PHN and CRPS afflicted skin revealed a unique and substantial increase in keratinocyte CGRP-IL within the painful sites of PHN and CRPS subjects. In control subjects, CGRP-IL was varied among epidermal keratinocytes, appearing typically at low to moderate levels, and being largely distributed heterogeneously among midlevel stratum spinosum keratinocytes (Fig. 1A,B; between arrows). As shown in supplementary Figure S1, CGRP-IL was observed among keratinocytes throughout the full thickness of the epidermis in lateral foot biopsies of both the diabetic and nondiabetic subjects. The immunolabeling varied from subject to subject but was not consistently different between the diabetic and non-diabetic biopsies.

In PHN patients, CGRP-IL was always more intensely expressed among keratinocytes in all painful PHN skin compared to nonpainful contralateral mirror-image locations (Fig. 1, compare C and D, E and F, G and H). Due to the increased levels of CGRP-IL, the keratinocytes in the painful skin are individually more clearly discernable than in control skin. The increased CGRP-IL in PHN skin was also very homogeneous among keratinocytes across the full thickness of the epidermis, with the exception of stratum basalis where the keratinocytes had moderate CGRP-IL. In the nonpainful contralateral skin of PHN subjects, CGRP-IL ranged mostly from low to moderate intensity, mostly being heterogeneously expressed among keratinocytes. However, the labeled keratinocytes were more widespread through the thickness of the epidermis compared to control subjects (Fig. 1A,B). The images presented in Figure 1 depict the *most* intense CGRP-IL among controls (A,B) observed, whereas in those images comparing PHN and contralateral skin, the images depict the *least* difference between the two sides observed among the PHN subjects.

As shown in Figures 1E–G, keratinocyte labeling was far less intense with monoclonal anti-human CGRPα (E,F) as compared with polyclonal anti-human CGRPα, even with a higher camera sensitivity to capture the monoclonal images. At this higher camera sensitivity, the innervation appears to be more intensely labeled with the monoclonal antibody, but the innervation labeling is actually comparable for both antibodies at the same camera settings (not shown). As is noted below, qPCR assays revealed that the human keratinocytes CGRP appears to be ~90% CGRPβ and 10% CGRPα. An enzyme immunoassay of comparable dilution series of synthesized human CGRPα and CGRPβ revealed that the monoclonal anti-human CGRPα was less sensitive in detecting CGRPβ than CGRPα (supplementary data). Thus, the more intense labeling of keratinocytes with the polyclonal anti-CGRP is likely due to the detection of a mix of 90% CGRPβ and 10% CGRPα, as well as their prepeptides, whereas the monoclonal CGRPα antibody may be preferentially labeling only the 10% CGRPα (see Fig. 7 and supplementary data).

In CRPS skin from hypothenar or lateral foot, CGRP-IL was consistently much higher compared with control (Fig. 1I–L). Additionally, note across each disorder, a decrease in detectable CGRP-IL of upper dermal nerves, as indicated by arrowheads. Similar to other published results [37,83], the PHN cohort had a consistent loss of PGP-IL epidermal endings in both active rash and ipsilateral sites compared with contralateral mirror-image sites (Fig. 1N), whereas the healthy controls showed no lateral differences (Fig. 1M). Because both of these disorders involve inflammatory activity, and CGRP has been implicated in neurogenic inflammation processes, we hypothesize that keratinocyte-derived CGRPβ may contribute to these severe chronic pain conditions.

Direct Nerve Injury: Spinal Nerve Ligation and Chronic Constriction—A prominent role of CGRP in spinal cord dorsal horn and peripheral tissues following experimental models of neuropathic pain has been hypothesized [67], however the peripheral source was considered to be neurogenic. In order to determine if keratinocyte-derived CGRP might also be playing a role in neuropathic pain conditions, two animal models of direct nerve injury were utilized. CGRP-IL in epidermal keratinocytes was increased following direct nerve injury in rats at times that corresponded with neuropathic pain behaviors (Fig. 2A, B). Following SNL at 30 and 60 days, mechanical allodynia was evident (Fig. 2A), and following CCI at 3, 7, and 14 days thermal hyperalgesia was observed (Fig. 2B). Utilizing the SNL and CCI models of neuropathic pain, hindpaw skin was processed for combinations of CGRP, NF, and/or PGP immunofluorescence. Control, unoperated rats (Fig. 2C,D) show strong CGRP-IL among axons of dermal nerves and axon terminals in the epidermis and around dermal blood vessels. In the epidermis, CGRP-IL was faint and heterogeneously expressed among suprabasal keratinocytes of the volar pad crown (Fig. 2C) and flat glabrous skin (Fig. 2D). By 30 days following SNL, a nearly complete loss of neural innervation is observed, while epidermal keratinocyte CGRP-IL appears more extensive throughout the pad crown (Fig. 2E) and flat (Fig. 2F) glabrous hindpaw skin. By 60 days following SNL, neural innervation has begun to return, but without a CGRP-IL contingent, whereas the epidermal keratinocyte CGRP-IL remains elevated among pad crown (Fig. 2G) and flat (Fig. 2H) glabrous hindpaw skin.

For CCI, naïve animals stood with normal posture to include full weight bearing on the entire flattened glabrous hindpaw, and had normal ranged thermal response latencies. Sham operated animals demonstrated no abnormalities in posture and had thermal withdrawal latencies of ipsilateral and contralateral hindpaws similar to the naïve animals. The CCI group showed significant decreases in withdrawal latency of the ipsilateral hindpaw compared with the naïve or sham operated animals beginning at 3 days after the surgery up to the end of the experiment (day 14; Fig. 2B). The posture of the CCI animals was compromised, having the foot held in an "antalgic posture" where the glabrous sole of the

ipsilateral hindpaw was not completely placed on the floor, nor was full weight bearing apparent. Sham operated animals (ipsilateral), had relatively normal appearing epidermal keratinocyte CGRP-IL, observed heterogeneously and low in level among suprabasal keratinocytes, along with several CGRP-IL nerve fibers throughout the dermis and epidermis (Fig. 2I). Similarly, robust PGP-IL among innervation of the dermis and epidermis appeared normal (Fig. 2J). Double label analysis for CGRP/PGP demonstrated normal appearing nerve bundles with numerous PGP axons (Fig. 2K, green plane), of which ~30% appeared with CGRP-IL (Fig. 2K, red plane), and double labeling for NF/PGP demonstrated normal robust NF-IL among large caliber fibers within dermal nerves (Fig 2L, red plane). Following CCI, an increase in keratinocyte CGRP-IL was observed (Fig. 2M), with a concomitant decrease in CGRP-IL among innervation. Very similar keratinocyte results can be seen upon inspection of the results from a similar nerve injury model investigating skin innervation of lower lip, however the authors did not address keratinocyte CGRP expression [47]. Similarly, a dramatic loss of PGP-IL innervation is evident among the dermis and epidermis (Fig. 2N). Double labeling for CGRP/PGP demonstrates an apparent increase in CGRP-IL within the dermal nerves (Fig. 2O, red plane; compare to Fig. 2K, red plane), but was mostly distributed among vacuolated cells affiliated with the larger caliber axons. Concomitantly, NF-IL is severely depleted among the large caliber axons within the deep nerves, indicating axons deterioration, and the likelihood that the vacuolated cells may be reactive Schwann cells (P, red panel) [15]. Taken altogether, these findings indicate that following proximal spinal nerve or more distal peripheral nerve injury, increased CGRP-IL among epidermal keratinocytes is present concomitant with decreased CGRP-IL of cutaneous innervation.

Inflammation Models: Complete Freund's Adjuvant (CFA) and Simian Immunodeficiency Virus (SIV)—CGRP is known to contribute to painful inflammatory conditions, and the source is largely considered to be neural [9,17]. In order to determine if keratinocyte-derived CGRP might also contribute to inflammatory pain, the CFA hindpaw direct inflammation model was used. Following CFA injection into the hindpaw of rat, CGRP-IL was increased among hindpaw epidermal keratinocytes by 3 days and remained elevated at 14 days after injection, with a concomitant decrease of CGRP-IL axons among the epidermis, dermal vasculature, and dermal nerves (Fig. 3A–D). Control uninjected rats displayed strong CGRP-IL of axonal innervation among the epidermal endings and subepidermal plexus, whereas epidermal keratinocyte CGRP-IL appears heterogeneous and weak among the volar pad crown. Similarly, the innervation to dermal vasculature and axons within dermal nerves appeared healthy and complete (Fig. 3A', A"). However, as soon as 2 hr following direct CFA injection, increased CGRP-IL was apparent among epidermal keratinocytes (Fig. 3B), with little change among the innervation of the epidermis, subepidermal plexus, dermal vasculature or in the composition of dermal nerves (Fig. 3B', B"). Continuing at 3 days after CFA injection, epidermal CGRP-IL was increased among superbasal keratinocytes (Fig. 3C), while neural innervation appeared depleted (i.e., lack of CGRP-IL or PGP-IL axon staining) from the epidermis and subepidermal plexus. Interestingly, among the dermal vasculature, a dramatic loss of CGRP-IL vascular adventitial innervation was observed, although PGP-IL axons were still present, and dermal nerves appeared distraught, with ragged PGP-IL and limited CGRP-IL axons present (Fig. 3C', C"). At 14 days after CFA, epidermal CGRP-IL remained elevated among the superbasal keratinocytes (Fig. 3D), while CGRP-IL axons were absent from the epidermis or subepidermal plexus. Dermal vasculature remained without CGRP-IL innervation among the vascular adventitial layers, although PGP-IL axons were still present, and dermal nerves remained distraught in appearance with limited CGRP-IL axons (Fig. 3D', D"). These findings indicate that following local direct inflammatory injury, alterations of both

epidermal immunochemistry and distal cutaneous innervation and are evident, including specifically an increase in CGRP-IL among keratinocytes.

In order to determine if direct skin inflammation was essential for the elevated CGRP-IL among keratinocytes, we used the CD8+ T-lymphocyte depletion SIV-infection rhesus model of AIDS, which results in rapid disease progression with high systemic viral loads and abundant inflammation. Rhesus macaques were infected with SIVmac251, monitored for signs of disease progression, and sacrificed upon the development of AIDS. Euthanasia was performed based on the following criteria; including extreme weight loss, documented opportunistic infection, persistent anorexia, severe intractable diarrhea, progressive neurologic sign or significant cardiac or pulmonary signs (Table 2). A single, uninfected monkey was used to collect control hypothenar region skin samples for comparison, and additional control tissue was also examined from normal monkeys analyzed in a prior study of naturally-occurring type 2 diabetes [77]. As depicted in Fig. 4A–E, all infected animals showed some degree of increased CGRP-IL among the hypothenar region epidermal keratinocytes. Importantly, not all animals had the same degree of CGRP-IL, consistent with the fact that they had different rates of disease progression with varying degrees of severity. Additionally, note the presence of detectable epidermal CGRP-IL axons within the skin of the animal with the least increase in epidermal keratinocytes CGRP-IL (Fig. 4D, arrows). Together, these findings demonstrate that inflammation, both cutaneous and systemic, can lead to an increase in CGRP-IL among epidermal keratinocytes.

Transgenic over-expression of noggin or BMP4 alters epidermal keratinocyte CGRP-IL and mRNA levels in vivo—Continuing to question the potential functions of CGRP in keratinocytes, we made use of a pair of previously investigated transgenic mice lines, which over-produce noggin or BMP-4 driven off of the K14 promoter. The noggin/BMP4 signaling system is essential for driving precursor cell lineages to either keratinocyte or neuronal fates. By manipulating these systems, we hypothesized that we might alter the CGRP-IL, and possible genetic regulating mechanisms, among epidermal keratinocytes. Hindpaw skin from adult transgenic mice was removed and immunolabeled for CGRP. Noggin over-expression resulted in high levels of CGRP-IL in epidermal keratinocytes among the volar pad crown (Fig. 5A) and flat (Fig. 5B) glabrous hindpaw skin. This keratinocyte CGRP-IL was more extensive and homogeneous throughout the superbasal layers. In contrast, BMP4 over-expression resulted in low levels of CGRP-IL in epidermal keratinocytes among the volar pad crown and flat glabrous hindpaw skin compared with the noggin animals (Fig. 5C, D), a pattern which more closely resembles that observed in wild-type strains (data not shown). As shown in a prior study, CGRP-IL on nerve fibers was present in the skin of both noggin and BMP-4 overexpressing mice although differences were detected among subtypes of CGRP-positive fibers [48]. These results demonstrate that the expression of CGRP in epidermal keratinocytes can be manipulated with the BMP4 system, and that over-expression of the noggin gene might act to be "neuralizing" the keratinocytes.

To confirm our CGRP-IL results, we then proceeded to use glabrous skin epidermis obtained by laser capture microdissection from BMP4- or noggin- overexpression transgenic mice. Total mRNA was obtained from a pool of 5–7 etched epidermis strips per sample, and processed for transcriptome array analysis, and quantitative PCR with primers specific to CGRPα, CGRPβ, BMP4, noggin, CRLR, RAMP1, and RCP (Invitrogen). The microarray analysis demonstrated positive results for both isoforms of CGRP and for the CGRP receptor system, CRLR, RAMP1, and RCP, and yielded 98 transcripts that were differentially expressed between both conditions, with 51 being overexpressed in the BMP4 mice and 47 overexpressed in the noggin mice (Supplementary Table 2; Gene Expression Omnibus GSE26231). In order to determine precise levels of mRNA for the CGRP

isoforms, qPCR was performed. Normalized mRNA levels, relative to the reference gene GAPDH, demonstrate a significant increase in both CGRPα and CGRPβ isoforms among the Noggin-overexpressing epidermal keratinocytes compared with the BMP4 over-expressing epidermal keratinocytes (Fig. 6A, asterisks). Additionally, dilution series analysis was used to confirm primer efficiency equality between the CGRPα and CGRPβ primer sets. Therefore, direct comparisons between CGRPα and CGRPβ expression from each transgenic animal were performed, and demonstrate that in both animals, CGRPβ is the significantly dominate isoform expressed, being ~3.5-fold more than the CGRPα isoform among both lines of transgenic animals (Fig. 6A, pound signs). These results demonstrate the existence of CGRP isoform mRNA in epidermal keratinocytes, and supports the validity of increased CGRP-IL observed among keratinocytes from transgenic mice, nerve injured rats, inflammatory-injured rats and monkeys, and in human clinical pain conditions.

Differentiation of keratinocytes in vitro alters CGRP and cognate receptor component mRNA levels—Various CGRP effects on keratinocytes have been described [60,100,104,106], however direct expression of CGRP among keratinocytes has not been previously reported. We used normal human epidermal keratinocytes (NHEK) grown as monolayer cultures and primary human keratinocytes grown as raft cultures at the air interface, allowing for stratification and formation of an organotypic pseudoepidermis (3D Raft), to further investigate the expression of CGRP in keratinocytes. Quantitative PCR analysis demonstrated that the degree of keratinocyte differentiation significantly increased the production of both CGRP mRNA isoforms compared with undifferentiated NHEK cells (Fig. 6B, asterisk). Furthermore, the data demonstrates that the 3D Raft cultures contain ~4-fold greater amounts of CGRP mRNA than $CaCl_2$ differentiation or undifferentiated cells *in vitro*, and importantly, that the CGRPβ isoform is expressed in undifferentiated NHEK (10.4-fold increase), differentiated NHEK (8.0-fold increase), and 3D raft cultures (12.3 folds higher), to a greater degree than the CGRPα isoform (Fig. 6B, pound signs). The receptor signaling system for the neuropeptide CGRP includes a promiscuous and specific receptor pairing (CRLR, RAMP1, respectively) and an essential adaptor protein, RCP. Results from qPCR analysis demonstrated variable expression for each of these components without clean distinction between the various differentiated states, but with organotypic cultures showing significant increases in both CRLR and RCP (Fig. 6C).

Keratinocytes in vitro express detectable CGRP pre-peptide—To further demonstrate the presence of active CGRP peptide in keratinocytes, cultures were subjected to Western Blot analysis. Using total protein samples from monolayer primary mouse keratinocyte cultures, a low level detectable band was observed from all samples at the predicted weight of CGRP precursor protein (Fig. 7A; 16kDa, arrows). The positive control CGRPα was detected at the processed size (~3.7kD), however, among the *in vitro* cultures, no mature peptide was detectable. Utilizing total protein from primary mouse fibroblast cultures (FB) as a negative control, immortalized and undifferentiated mouse keratinocyte monolayer cultures (MK116), and freshly dissociated and homogenized mouse trigeminal ganglia tissue (TG) as a positive control, the MK116 and TG showed definitive bands at the predicted weight of CGRP precursor protein, while no band was detectable in the FB lane (Fig 7B; 16kDa, arrow). To determine if CGRP protein was detectable in human keratinocyte cultures, total protein samples from organotypic human keratinocytes (3D raft cultures) were utilized. A detectable band corresponding to the predicted molecular weight of the CGRP precursor protein was observed in all lanes (Fig. 7C; 16kD, arrow). To test the specificity of the anti-CGRP polyclonal antibody used to probe each Western membrane, CGRPα (1µg) and total protein samples from mouse trigeminal ganglia (TG, positive control) and mouse fibroblasts (FB, negative control) were run in duplicate, and the membrane separated. One half of the membrane (left) was probed with anti-CGRP (Rb

polyclonal, 1:2000; Chemicon Inc, Temecula, CA), while the other half (right) was probed with a pre-adsorbed anti-CGRP antibody mix. Mature CGRP (~3.7kD) and CGRP precursor protein (16kD; arrows) bands were detected on the left membrane lanes 1 and 2, but not 3. However, no bands were detectible on the right membrane after specific primary antibody pre-adsorption (Figure 7D, 16kDa, arrow), demonstrating evidence for the specificity of the antibody.

Thermal stimulus release of CGRP from cultured keratinocytes—Prior studies indicated that heating the skin causes a release of CGRP from peptidergic CGRP-positive endings in the skin. We sought to determine whether thermal stimulation of keratinocytes would also result in a release of CGRP. An initial assessment of thermally stimulated MK-116 mouse keratinocytes using the available EIA kit plated with monoclonal anti-human CGRPα indicated a release of CGRP with a 48°C stimulus (supplemental Fig. S2, top graph). As well, following 48 °C thermal challenge, CGRP-IR was decreased, indicating a potential release event (supplemental Fig. S2, bottom panels). However, subsequent attempts utilizing human cells failed to replicate the EIA detectable release. Importantly, it has been noted that manufacturer changes to the EIA kit during the interim between attempts at replication documented loses in sensitivity, findings that were replicated in our experiments based upon the detection limits of the generated standard curves (data not shown). Additional EIA experimental results also indicated that the human anti-CGRPα is less sensitive for detecting the CGRPβ isoform at concentrations below 500 pg/mL (Supplemental Fig. S3).

Discussion

CGRP is a potent vasodilatory peptide whose signaling has been implicated in normal cutaneous non-noxious and noxious thermal sensation, vasodilation and thermal regulation [80], as well as in epidermal homeostasis, including keratinocyte proliferation and cytokine expression, and the regulation of melanocytes and Langerhans cells [25,34,45,53,87,92,99,106,109,111]. CGRP has also been implicated in pathologic conditions including neurogenic inflammation, chronic pain associated with peripheral neuropathies, migraine headaches, musculoskeletal pain associated with vasculature, and painful puritic dermatopathies such as psoriasis, a condition associated with epidermal keratinocyte dysfunction [5,9,46,55,73,86,91].

Various experimentally-induced and naturally occurring neuropathic conditions have been shown to be associated with increases in CGRP levels in the skin, in blood and/or in CSF [14,72]. These increases are attributed primarily to neurogenic CGRP release from central terminals or sensory endings of peptidergic subsets of C and Aδ fibers that innervate tissues throughout the body, especially epidermis and vasculature [3,16,40–41,77,89]. While CGRP functions as a neurotransmitter for peptidergic fiber terminals in the CNS, antidromic activity releases CGRP from peripheral sensory endings, resulting in neuro-effector impacts such as vasodilation [13,52,90,116]. Under normal conditions, peptidergic fibers likely have different sensory functions related to where their sensory endings terminate and to the combination and proportions of various types of receptors and ion channels that they co-express. Potentially, these same receptors and ion channels may directly mediate CGRP release from sensory endings in response to local tissue interaction or interactions with other types of sensory or autonomic innervation. For example, a large proportion of CGRP-IL neurons express TrpV1 and innervate the epidermis and blood vessels [3–4,83,88]. TrpV1 is activated by painfully high temperature, low pH, and extraneous capsaicin and can be functionally modulated by intrinsic endocannabinoids [2,21–22,42,54,105]. Peptidergic neurons also widely express acid sensing ion channels (ASICs), with subsets of vascular peptidergic endings expressing the ASIC3 receptor which is preferentially activated by lactic

acid and possibly mechanical stimulation [68,75,84,108]. At least some vascular CGRP endings express adrenergic receptors that may be activated by noradrenergic release from intermingled sympathetic terminals mediating vasoconstriction [56]. Other peptidergic innervation expresses purinergic receptors responsive to ATP, and voltage-gated ion channels such as NaV1.7 [33]. Moreover, peptidergic endings in the epidermis have been shown to express µ-opioid receptors and GIRK channels that may inhibit their depolarization [57] and peptidergic Aδ fibers express the histamine receptor 3 that may block the release of CGRP [19]. Taken altogether, these data demonstrate that neurogenic release of CGRP from sensory endings for normal functions is likely regulated by complex local interactions. Under pathological conditions, alterations of any of these regulated mechanisms may result in increased CGRP levels, thereby exacerbating inflammatory and painful responses.

Herein, we document that keratinocytes also express CGRP-IL which is increased in painful skin from humans with PHN (see also Fig. 2 in Petersen et al., 2002) and CRPS type 1, as well as in animal models of inflammatory and nerve injury induced pain. Interestingly, such an increase was not consistently evident among diabetics with painful neuropathy, perhaps because of the relatively slow incipient nature of the disease. The presence of CGRP-IL among keratinocytes, even in normal skin, adds to a long list of neurochemical properties that are expressed by keratinocytes [11,44,65,102,113]. Keratinocytes are derived from the same embryonic ectoderm layer that gives rise to nearly all the neurons of the peripheral and central nervous system. During development, the ectoderm generates keratinocytes through BMP4 signaling which is blocked by the release of noggin from the notochord to induce the formation of neurons [66]. We previously demonstrated that BMP4/noggin interactions later regulate the proportions of epidermal innervation by using lines of transgenic mice where a K14 promoter sequence induced excess expression of BMP4 or noggin in basal keratinocytes [48]. Herein, we document that noggin overexpression also increases CGRP expression in keratinocytes, indicating that TGFβ interactions are likely regulators of epidermal neurochemical properties.

Largely, the wide variety of neurochemical properties detected among keratinocytes have been described in relation to epidermal barrier function, wound healing, and skin homeostasis, particularly in regulating keratinocyte proliferation and differentiation, and owing that keratinocytes are considered to be non-depolarizing cells. Consistent with observations that CGRP has direct effects on keratinocytes, including proliferation, our results confirm that keratinocytes express mRNA for the CGRP receptor complex proteins, CRLR, RAMP1, and RCP. Thus, keratinocytes may be regulated by neurogenic release of CGRP from peptidergic sensory endings in the epidermis. However, our results also indicate that the keratinocytes themselves are a source of CGRP which may regulate autocrine/paracrine interactions involved in normal epidermal homeostasis, and therefore also have the potential to be altered under pathological conditions, for example psoriasis. Psoriasis is a disease characterized by inflammation and hyperproliferation of keratinocytes in the skin. Overexpression of CGRP in lesions of psoriasis patients has been noted [55], and studies done by Yu et al. (2009) have suggested that these increases in keratinocyte proliferation are due to the presence of CGRP [114].

Importantly, recent evidence is increasingly indicating that the neurochemical properties in keratinocytes are directly involved in sensory transduction and the release of neurotransmitters that can activate or modulate the function of sensory endings. Traditionally, sensory transduction is thought to start from direct stimulation of peripheral nerve terminals, but this is not necessarily the only, or even the principle, mechanism (for a systemic review, refer to Dussor et al, 2009). Epidermal keratinocytes have been shown to release β-endorphin, which ameliorates heat-pain hind paw withdrawal most likely by

binding to μ-opioid receptors located on CGRP containing sensory endings in the epidermis [57]. Voltage-gated sodium channels are expressed on keratinocytes, and are involved in ATP release which may contribute to pain by activating purinergic receptors located primarily on nonpeptidergic sensory endings [33,117]. In addition, TRPV3, a warm and heat sensitive channel, is expressed on keratinocytes, but not on primary sensory neurons in mice [24,82]. However, behavioral studies showed that both warm and heat sensations were impaired in TRPV3 mutant mice [29,69]. Thus, this impairment may be due to a defect in keratinocyte function rather than a defect in sensory ending transduction. Furthermore, we have previously documented that CRPS type1 and PHN are accompanied by a dramatic increase in NaV immunolabeling in epidermal keratinocytes, indicating that pathologies in the epidermal chemistry may also be contributors to chronic pain [117]. Our results indicate that an increase in CGRP in keratinocytes in these human diseases and in the experimental rat models of induced pain may also be a contributor to neuropathic pain. Surprisingly, the experimental nerve injury results indicate that the increase in keratinocyte CGRP-IL does not require a local inflammatory cascade.

In some regions where both CGRPα and CGRPβ are expressed, such as the sensory ganglion, CGRPα is the predominant form [74]. By contrast, our transcriptomic and qPCR data indicate that the keratinocyte CGRP is predominantly the CGRPβ isoform. CGRP pre-peptide and significant mRNA expression for both CGRPβ and CGRPα were consistently detected in mouse and human keratinocyte cultures with greater levels in the more differentiated multi-layer cultures than the monolayer cultures. CGRP-IL increased dramatically and mRNA levels for CGRPβ and CGRPα increased significantly in the epidermis of the noggin compared to BMP4 overexpressing mice. In all cases, mRNA expression for CGRPβ was several fold higher than that for CGRPα, especially in differentiated human keratinocyte raft cultures. The two isoforms in humans differ by three amino acids in the 3, 22 and 25 positions [70,111] and are believed to largely function in a similar manner. However, they are differentially expressed during development, and locations expressing predominately a single isoform are known [71,74,109,111]. Although the two isoforms of CGRP are believed to largely function in a similar manner, several instances where biologic discriminations can be found have been demonstrated [63,93,97,107]. Thus, the keratinocyte-derived CGRPβ may be a differential signal from CGRPα released from nerve terminals. Importantly, these isoforms are derived from separate genes, albeit on the same chromosome [97], indicating that CGRP isoforms may be independently regulated for keratinocyte and neuron mediated functions under normal and pathological conditions. Conceivably, CGRPβ produced by keratinocytes may contribute to elevated levels of CGRP in the painful skin of humans with CRPS and of rats injected subcutaneously with CFA or stimulated with capsaicin, but the assays used in those studies did not distinguish between different isoforms [9,46,58,73,97–98].

In conclusion, our results suggest the presence of differential expression of the two isoforms of CGRP, with CGRPβ dominating in keratinocytes and CGRPα dominating in sensory neurons. The differential expression and regulation of the isoforms may be a detectable signal involved in sensory transduction and modulation, as well as in regulating epidermal homeostasis. The observed increases in CGRP-IL among epidermal keratinocytes from human, monkey, and rat pain conditions, indicates that epidermally-derived CGRPβ may contribute to chronic pain mechanisms. Given that the CGRPα and CGRPβ isoforms are derived from separate genes and are differentially produced in keratinocytes and neurons (demonstrating that that they are separately regulated), further indicates that the isoforms may differentially contribute to both homeostatic maintenance and chronic pain conditions such as PHN, CRPS, migraine headache and psoriasis. Importantly, these results also imply that the CGRP isoforms may be specifically targeted for disease therapeutics.

Summary

CGRP is a potent vasodilatory neuropeptide that contributes to a variety of normal sensory, vasoregulatory, and epidermal functions, but which is also implicated in a variety of chronic pain conditions where it is expressed at high levels in the skin, blood, and CSF. The source of the increased CGRP has been attributed to peptidergic sensory innervation which synthesizes and releases primarily the CGRPα isoform. Our results reveal that much of the increase may be due to the CGRPβ isoform made by epidermal keratinocytes which express high levels of CGRP immunoreactivity in a variety of human and animal chronic pain conditions.

Supplementary Material

Refer to Web version on PubMed Central for supplementary material.

Acknowledgments

References

1. Ai X, Cappuzzello J, Hall AK. Activin and bone morphogenetic proteins induce calcitonin gene-related peptide in embryonic sensory neurons in vitro. Mol Cell Neurosci. 1999; 14:506–518. [PubMed: 10656256]

2. Akopian AN, Ruparel NB, Patwardhan A, Hargreaves KM. Cannabinoids desensitize capsaicin and mustard oil responses in sensory neurons via TRPA1 activation. J Neurosci. 2008; 28:1064–1075. [PubMed: 18234885]

3. Albrecht PJ, Hines S, Eisenberg E, Pud D, Finlay DR, Connolly MK, Pare M, Davar G, Rice FL. Pathologic alterations of cutaneous innervation and vasculature in affected limbs from patients with complex regional pain syndrome. Pain. 2006; 120:244–266. [PubMed: 16427199]

4. Albrecht PJ, Rice FL. Role of small-fiber afferents in pain mechanisms with implications on diagnosis and treatment. Curr Pain Headache Rep. 2010; 14:179–188. [PubMed: 20425194]

5. Ambalavanar R, Dessem D, Moutanni A, Yallampalli C, Yallampalli U, Gangula P, Bai G. Muscle inflammation induces a rapid increase in calcitonin gene-related peptide (CGRP) mRNA that temporally relates to CGRP immunoreactivity and nociceptive behavior. Neuroscience. 2006; 143:875–884. [PubMed: 17027165]

6. Ambalavanar R, Yallampalli C, Yallampalli U, Dessem D. Injection of adjuvant but not acidic saline into craniofacial muscle evokes nociceptive behaviors and neuropeptide expression. Neuroscience. 2007; 149:650–659. [PubMed: 17928159]

7. Arulmani U, Maassenvandenbrink A, Villalon CM, Saxena PR. Calcitonin gene-related peptide and its role in migraine pathophysiology. Eur J Pharmacol. 2004; 500:315–330. [PubMed: 15464043]

8. Bai G, Wei D, Zou S, Ren K, Dubner R. Inhibition of class II histone deacetylases in the spinal cord attenuates inflammatory hyperalgesia. Mol Pain. 2010; 6:51. [PubMed: 20822541]

9. Benemei S, Nicoletti P, Capone JG, Geppetti P. CGRP receptors in the control of pain and inflammation. Curr Opin Pharmacol. 2009; 9:9–14. [PubMed: 19157980]

10. Bennett GJ, Xie YK. A peripheral mononeuropathy in rat that produces disorders of pain sensation like those seen in man. Pain. 1988; 33:87–107. [PubMed: 2837713]

11. Bigliardi PL, Buchner S, Rufli T, Bigliardi-Qi M. Specific stimulation of migration of human keratinocytes by mu-opiate receptor agonists. J Recept Signal Transduct Res. 2002; 22:191–199. [PubMed: 12503615]

12. Bileviciute I, Stenfors C, Theodorsson E, Lundeberg T. Unilateral injection of calcitonin gene-related peptide (CGRP) induces bilateral oedema formation and release of CGRP-like immunoreactivity in the rat hindpaw. Br J Pharmacol. 1998; 125:1304–1312. [PubMed: 9863661]

13. Birklein F, Schmelz M. Neuropeptides, neurogenic inflammation and complex regional pain syndrome (CRPS). Neurosci Lett. 2008; 437:199–202. [PubMed: 18423863]

14. Birklein F, Schmelz M, Schifter S, Weber M. The important role of neuropeptides in complex regional pain syndrome. Neurology. 2001; 57:2179–2184. [PubMed: 11756594]

15. Bove GM, Light AR. Calcitonin gene-related peptide and peripherin immunoreactivity in nerve sheaths. Somatosens Mot Res. 1995; 12:49–57. [PubMed: 7571942]

16. Bowsher D, Geoffrey Woods C, Nicholas AK, Carvalho OM, Haggett CE, Tedman B, Mackenzie JM, Crooks D, Mahmood N, Twomey JA, Hann S, Jones D, Wymer JP, Albrecht PJ, Argoff CE, Rice FL. Absence of pain with hyperhidrosis: a new syndrome where vascular afferents may mediate cutaneous sensation. Pain. 2009; 147:287–298. [PubMed: 19836135]

17. Brain SD, Williams TJ. Inflammatory oedema induced by synergism between calcitonin gene-related peptide (CGRP) and mediators of increased vascular permeability. Br J Pharmacol. 1985; 86:855–860. [PubMed: 2416378]

18. Burdo TH, Soulas C, Orzechowski K, Button J, Krishnan A, Sugimoto C, Alvarez X, Kuroda MJ, Williams KC. Increased monocyte turnover from bone marrow correlates with severity of SIV encephalitis and CD163 levels in plasma. PLoS Pathog. 2010; 6:e1000842. [PubMed: 20419144]

19. Cannon KE, Chazot PL, Hann V, Shenton F, Hough LB, Rice FL. Immunohistochemical localization of histamine H3 receptors in rodent skin, dorsal root ganglia, superior cervical ganglia, and spinal cord: potential antinociceptive targets. Pain. 2007; 129:76–92. [PubMed: 17134835]

20. Carleson J, Lundeberg T, Appelgren B. Muscle and brain changes of calcitonin gene-related peptide in experimentally induced unilateral rat masseter myositis. J Orofac Pain. 2004; 18:246–252. [PubMed: 15509004]

21. Caterina MJ, Julius D. The vanilloid receptor: a molecular gateway to the pain pathway. Annu Rev Neurosci. 2001; 24:487–517. [PubMed: 11283319]

22. Caterina MJ, Schumacher MA, Tominaga M, Rosen TA, Levine JD, Julius D. The capsaicin receptor: a heat-activated ion channel in the pain pathway. Nature. 1997; 389:816–824. [PubMed: 9349813]

23. Cheng J, Turksen K, Yu QC, Schreiber H, Teng M, Fuchs E. Cachexia and graft-vs.-host-disease-type skin changes in keratin promoter-driven TNF alpha transgenic mice. Genes Dev. 1992; 6:1444–1456. [PubMed: 1379563]

24. Chung MK, Lee H, Mizuno A, Suzuki M, Caterina MJ. TRPV3 and TRPV4 mediate warmth-evoked currents in primary mouse keratinocytes. J Biol Chem. 2004; 279:21569–21575. [PubMed: 15004014]

25. Cridland RA, Henry JL. Effects of intrathecal administration of neuropeptides on a spinal nociceptive reflex in the rat: VIP, galanin, CGRP, TRH, somatostatin and angiotensin II. Neuropeptides. 1988; 11:23–32. [PubMed: 2452992]

26. Denda M, Fujiwara S, Hibino T. Expression of voltage-gated calcium channel subunit alpha1C in epidermal keratinocytes and effects of agonist and antagonists of the channel on skin barrier homeostasis. Exp Dermatol. 2006; 15:455–460. [PubMed: 16689862]

27. Denda M, Tsutsumi M, Denda S. Topical application of TRPM8 agonists accelerates skin permeability barrier recovery and reduces epidermal proliferation induced by barrier insult: role of cold-sensitive TRP receptors in epidermal permeability barrier homoeostasis. Exp Dermatol. 2010; 19:791–795. [PubMed: 20636355]

28. Denda M, Tsutsumi M, Goto M, Ikeyama K, Denda S. Topical application of TRPA1 agonists and brief cold exposure accelerate skin permeability barrier recovery. J Invest Dermatol. 2010; 130:1942–1945. [PubMed: 20182443]

29. Dhaka A, Viswanath V, Patapoutian A. Trp ion channels and temperature sensation. Annu Rev Neurosci. 2006; 29:135–161. [PubMed: 16776582]

30. DiPersio CM, Shao M, Di Costanzo L, Kreidberg JA, Hynes RO. Mouse keratinocytes immortalized with large T antigen acquire alpha3beta1 integrin-dependent secretion of MMP-9/ gelatinase B. J Cell Sci. 2000; 113(Pt 16):2909–2911. [PubMed: 10910775]

31. Dlugosz AA, Cheng C, Williams EK, Darwiche N, Dempsey PJ, Mann B, Dunn AR, Coffey RJ Jr, Yuspa SH. Autocrine transforming growth factor alpha is dispensible for v-rasHa-induced epidermal neoplasia: potential involvement of alternate epidermal growth factor receptor ligands. Cancer Res. 1995; 55:1883–1893. [PubMed: 7728756]

32. Durham PL. Inhibition of calcitonin gene-related peptide function: a promising strategy for treating migraine. Headache. 2008; 48:1269–1275. [PubMed: 18808507]

33. Dussor G, Koerber HR, Oaklander AL, Rice FL, Molliver DC. Nucleotide signaling and cutaneous mechanisms of pain transduction. Brain Res Rev. 2009; 60:24–35. [PubMed: 19171165]

34. E Y, Golden SC, Shalita AR, Lee WL, Maes DH, Matsui MS. Neuropeptide (calcitonin gene-related peptide) induction of nitric oxide in human keratinocytes in vitro. J Invest Dermatol. 2006; 126:1994–2001. [PubMed: 16710309]

35. Eberhardt M, Hoffmann T, Sauer SK, Messlinger K, Reeh PW, Fischer MJ. Calcitonin gene-related peptide release from intact isolated dorsal root and trigeminal ganglia. Neuropeptides. 2008; 42:311–317. [PubMed: 18328558]

36. Ellington HC, Cotter MA, Cameron NE, Ross RA. The effect of cannabinoids on capsaicin-evoked calcitonin gene-related peptide (CGRP) release from the isolated paw skin of diabetic and non-diabetic rats. Neuropharmacology. 2002; 42:966–975. [PubMed: 12069907]

37. Fink E, Oaklander AL. Small-fiber neuropathy: answering the burning questions. Sci Aging Knowledge Environ. 2006; 2006:pe7. [PubMed: 16525192]

38. Fuchs E. Keratins and the skin. Annu Rev Cell Dev Biol. 1995; 11:123–153. [PubMed: 8689554]

39. Fuchs E, Byrne C. The epidermis: rising to the surface. Curr Opin Genet Dev. 1994; 4:725–736. [PubMed: 7531523]

40. Fundin BT, Arvidsson J, Aldskogius H, Johansson O, Rice SN, Rice FL. Comprehensive immunofluorescence and lectin binding analysis of intervibrissal fur innervation in the mystacial pad of the rat. J Comp Neurol. 1997; 385:185–206. [PubMed: 9268123]

41. Fundin BT, Pfaller K, Rice FL. Different distributions of the sensory and autonomic innervation among the microvasculature of the rat mystacial pad. J Comp Neurol. 1997; 389:545–568. [PubMed: 9421138]

42. Gavva NR, Bannon AW, Surapaneni S, Hovland DN Jr, Lehto SG, Gore A, Juan T, Deng H, Han B, Klionsky L, Kuang R, Le A, Tamir R, Wang J, Youngblood B, Zhu D, Norman MH, Magal E, Treanor JJ, Louis JC. The vanilloid receptor TRPV1 is tonically activated in vivo and involved in body temperature regulation. J Neurosci. 2007; 27:3366–3374. [PubMed: 17392452]

43. Getsios S, Simpson CL, Kojima S, Harmon R, Sheu LJ, Dusek RL, Cornwell M, Green KJ. Desmoglein 1-dependent suppression of EGFR signaling promotes epidermal differentiation and morphogenesis. J Cell Biol. 2009; 185:1243–1258. [PubMed: 19546243]

44. Grando SA, Zelickson BD, Kist DA, Weinshenker D, Bigliardi PL, Wendelschafer-Crabb G, Kennedy WR, Dahl MV. Keratinocyte muscarinic acetylcholine receptors: immunolocalization and partial characterization. J Invest Dermatol. 1995; 104:95–100. [PubMed: 7528248]

45. Granstein RD, Matsui MS. UV radiation-induced immunosuppression and skin cancer. Cutis. 2004; 74:4–9. [PubMed: 15603215]

46. Greco R, Tassorelli C, Sandrini G, Di Bella P, Buscone S, Nappi G. Role of calcitonin gene-related peptide and substance P in different models of pain. Cephalalgia. 2008; 28:114–126. [PubMed: 18197882]

47. Grelik C, Allard S, Ribeiro-da-Silva A. Changes in nociceptive sensory innervation in the epidermis of the rat lower lip skin in a model of neuropathic pain. Neurosci Lett. 2005; 389:140–145. [PubMed: 16139429]

48. Guha U, Gomes WA, Samanta J, Gupta M, Rice FL, Kessler JA. Target-derived BMP signaling limits sensory neuron number and the extent of peripheral innervation in vivo. Development. 2004; 131:1175–1186. [PubMed: 14973275]

49. Hargreaves K, Dubner R, Brown F, Flores C, Joris J. A new and sensitive method for measuring thermal nociception in cutaneous hyperalgesia. Pain. 1988; 32:77–88. [PubMed: 3340425]

50. Hennings H, Holbrook K, Steinert P, Yuspa S. Growth and differentiation of mouse epidermal cells in culture: effects of extracellular calcium. Curr Probl Dermatol. 1980; 10:3–25. [PubMed: 7238094]

51. Ho TW, Edvinsson L, Goadsby PJ. CGRP and its receptors provide new insights into migraine pathophysiology. Nat Rev Neurol. 2010

52. Holzer P. Neurogenic vasodilatation and plasma leakage in the skin. Gen Pharmacol. 1998; 30:5–11. [PubMed: 9457475]

53. Hosoi J, Murphy GF, Egan CL, Lerner EA, Grabbe S, Asahina A, Granstein RD. Regulation of Langerhans cell function by nerves containing calcitonin gene-related peptide. Nature. 1993; 363:159–163. [PubMed: 8483499]

54. Jeske NA, Patwardhan AM, Gamper N, Price TJ, Akopian AN, Hargreaves KM. Cannabinoid WIN 55,212-2 regulates TRPV1 phosphorylation in sensory neurons. J Biol Chem. 2006; 281:32879–32890. [PubMed: 16954222]

55. Jiang WY, Raychaudhuri SP, Farber EM. Double-labeled immunofluorescence study of cutaneous nerves in psoriasis. Int J Dermatol. 1998; 37:572–574. [PubMed: 9731999]

56. Kawasaki H, Nuki C, Saito A, Takasaki K. Role of calcitonin gene-related peptide-containing nerves in the vascular adrenergic neurotransmission. J Pharmacol Exp Ther. 1990; 252:403–409. [PubMed: 1688944]

57. Khodorova A, Navarro B, Jouaville LS, Murphy JE, Rice FL, Mazurkiewicz JE, Long-Woodward D, Stoffel M, Strichartz GR, Yukhananov R, Davar G. Endothelin-B receptor activation triggers an endogenous analgesic cascade at sites of peripheral injury. Nat Med. 2003; 9:1055–1061. [PubMed: 12847519]

58. Kilo S, Harding-Rose C, Hargreaves KM, Flores CM. Peripheral CGRP release as a marker for neurogenic inflammation: a model system for the study of neuropeptide secretion in rat paw skin. Pain. 1997; 73:201–207. [PubMed: 9415506]

59. Kim SH, Chung JM. An experimental model for peripheral neuropathy produced by segmental spinal nerve ligation in the rat. Pain. 1992; 50:355–363. [PubMed: 1333581]

60. Kiss M, Kemeny L, Gyulai R, Michel G, Husz S, Kovacs R, Dobozy A, Ruzicka T. Effects of the neuropeptides substance P, calcitonin gene-related peptide and alpha-melanocyte-stimulating hormone on the IL-8/IL-8 receptor system in a cultured human keratinocyte cell line and dermal fibroblasts. Inflammation. 1999; 23:557–567. [PubMed: 10565569]

61. Kress M, Guthmann C, Averbeck B, Reeh PW. Calcitonin gene-related peptide and prostaglandin E2 but not substance P release induced by antidromic nerve stimulation from rat skin in vitro. Neuroscience. 1999; 89:303–310. [PubMed: 10051237]

62. Kress, M.; Reeh, PW. Chemical Excitation and Sensitization in Nociceptors. In: Cervero, F.; Belmonte, C., editors. Neurobiology of Nociceptors. New York: Oxford UP; 1996. p. 258-297.

63. Li J, Zhang M, Yang C, Dun Y, Zhang Y, Hao Y. Nitroglycerin protects small intestine from ischemia-reperfusion injury via NO-cGMP pathway and upregulation of alpha-CGRP. J Gastrointest Surg. 2009; 13:478–485. [PubMed: 19002537]

64. Lumpkin EA, Caterina MJ. Mechanisms of sensory transduction in the skin. Nature. 2007; 445:858–865. [PubMed: 17314972]

65. Maccarrone M, Di Rienzo M, Battista N, Gasperi V, Guerrieri P, Rossi A, Finazzi-Agro A. The endocannabinoid system in human keratinocytes. Evidence that anandamide inhibits epidermal differentiation through CB1 receptor-dependent inhibition of protein kinase C, activation protein-1, and transglutaminase. J Biol Chem. 2003; 278:33896–33903. [PubMed: 12815050]

66. Marcelle C, Stark MR, Bronner-Fraser M. Coordinate actions of BMPs, Wnts, Shh and noggin mediate patterning of the dorsal somite. Development. 1997; 124:3955–3963. [PubMed: 9374393]

67. Mogil JS, Miermeister F, Seifert F, Strasburg K, Zimmermann K, Reinold H, Austin JS, Bernardini N, Chesler EJ, Hofmann HA, Hordo C, Messlinger K, Nemmani KV, Rankin AL, Ritchie J, Siegling A, Smith SB, Sotocinal S, Vater A, Lehto SG, Klussmann S, Quirion R, Michaelis M, Devor M, Reeh PW. Variable sensitivity to noxious heat is mediated by differential expression of the CGRP gene. Proc Natl Acad Sci U S A. 2005; 102:12938–12943. [PubMed: 16118273]

68. Molliver DC, Immke DC, Fierro L, Pare M, Rice FL, McCleskey EW. ASIC3, an acid-sensing ion channel, is expressed in metaboreceptive sensory neurons. Mol Pain. 2005; 1:35. [PubMed: 16305749]

69. Moqrich A, Hwang SW, Earley TJ, Petrus MJ, Murray AN, Spencer KS, Andahazy M, Story GM, Patapoutian A. Impaired thermosensation in mice lacking TRPV3, a heat and camphor sensor in the skin. Science. 2005; 307:1468–1472. [PubMed: 15746429]

70. Moskowitz MA, Cutrer FM. CGRP: blood flow and more? Cephalalgia. 1996; 16:287. [PubMed: 8869758]

71. Mulderry PK, Ghatei MA, Spokes RA, Jones PM, Pierson AM, Hamid QA, Kanse S, Amara SG, Burrin JM, Legon S, et al. Differential expression of alpha-CGRP and beta-CGRP by primary sensory neurons and enteric autonomic neurons of the rat. Neuroscience. 1988; 25:195–205. [PubMed: 2839796]

72. Nahin RL, Byers MR. Adjuvant-induced inflammation of rat paw is associated with altered calcitonin gene-related peptide immunoreactivity within cell bodies and peripheral endings of primary afferent neurons. J Comp Neurol. 1994; 349:475–485. [PubMed: 7852637]

73. Neugebauer V, Rumenapp P, Schaible HG. Calcitonin gene-related peptide is involved in the spinal processing of mechanosensory input from the rat's knee joint and in the generation and maintenance of hyperexcitability of dorsal horn-neurons during development of acute inflammation. Neuroscience. 1996; 71:1095–1109. [PubMed: 8684614]

74. Noguchi K, Senba E, Morita Y, Sato M, Tohyama M. Alpha-CGRP and beta-CGRP mRNAs are differentially regulated in the rat spinal cord and dorsal root ganglion. Brain Res Mol Brain Res. 1990; 7:299–304. [PubMed: 2163005]

75. Olson TH, Riedl MS, Vulchanova L, Ortiz-Gonzalez XR, Elde R. An acid sensing ion channel (ASIC) localizes to small primary afferent neurons in rats. Neuroreport. 1998; 9:1109–1113. [PubMed: 9601677]

76. Opree A, Kress M. Involvement of the proinflammatory cytokines tumor necrosis factor-alpha, IL-1 beta, and IL-6 but not IL-8 in the development of heat hyperalgesia: effects on heat-evoked calcitonin gene-related peptide release from rat skin. J Neurosci. 2000; 20:6289–6293. [PubMed: 10934280]

77. Pare M, Albrecht PJ, Noto CJ, Bodkin NL, Pittenger GL, Schreyer DJ, Tigno XT, Hansen BC, Rice FL. Differential hypertrophy and atrophy among all types of cutaneous innervation in the glabrous skin of the monkey hand during aging and naturally occurring type 2 diabetes. J Comp Neurol. 2007; 501:543–567. [PubMed: 17278131]

78. Pare M, Elde R, Mazurkiewicz JE, Smith AM, Rice FL. The Meissner corpuscle revised: a multiafferented mechanoreceptor with nociceptor immunochemical properties. J Neurosci. 2001; 21:7236–7246. [PubMed: 11549734]

79. Pare M, Smith AM, Rice FL. Distribution and terminal arborizations of cutaneous mechanoreceptors in the glabrous finger pads of the monkey. J Comp Neurol. 2002; 445:347–359. [PubMed: 11920712]

80. Park TJ, Comer C, Carol A, Lu Y, Hong HS, Rice FL. Somatosensory organization and behavior in naked mole-rats: II. Peripheral structures, innervation, and selective lack of neuropeptides associated with thermoregulation and pain. J Comp Neurol. 2003; 465:104–120. [PubMed: 12926019]

81. Patthey C, Edlund T, Gunhaga L. Wnt-regulated temporal control of BMP exposure directs the choice between neural plate border and epidermal fate. Development. 2009; 136:73–83. [PubMed: 19060333]

82. Peier AM, Reeve AJ, Andersson DA, Moqrich A, Earley TJ, Hergarden AC, Story GM, Colley S, Hogenesch JB, McIntyre P, Bevan S, Patapoutian A. A heat-sensitive TRP channel expressed in keratinocytes. Science. 2002; 296:2046–2049. [PubMed: 12016205]

83. Petersen KL, Rice FL, Suess F, Berro M, Rowbotham MC. Relief of post-herpetic neuralgia by surgical removal of painful skin. Pain. 2002; 98:119–126. [PubMed: 12098623]

84. Petruska JC, Napaporn J, Johnson RD, Cooper BY. Chemical responsiveness and histochemical phenotype of electrophysiologically classified cells of the adult rat dorsal root ganglion. Neuroscience. 2002; 115:15–30. [PubMed: 12401318]

85. Price TJ, Flores CM. Critical evaluation of the colocalization between calcitonin gene-related peptide, substance P, transient receptor potential vanilloid subfamily type 1 immunoreactivities, and isolectin B4 binding in primary afferent neurons of the rat and mouse. J Pain. 2007; 8:263–272. [PubMed: 17113352]

86. Reich A, Orda A, Wisnicka B, Szepietowski JC. Plasma concentration of selected neuropeptides in patients suffering from psoriasis. Exp Dermatol. 2007; 16:421–428. [PubMed: 17437485]

87. Rezaeian AH, Isokane T, Nishibori M, Chiba M, Hiraiwa N, Yoshizawa M, Yasue H. alphaCGRP and betaCGRP transcript amount in mouse tissues of various developmental stages and their tissue expression sites. Brain Dev. 2009; 31:682–693. [PubMed: 19062206]

88. Rice, F.; Albrecht, P. Cutaneous Mechanisms of Tactile Perception: Morphological and Chemical Organization of the Innervation to the Skin. In: Basbaum, A., editor. The Senses: A comprehensive Reference, Vol 6, omatosensation. Vol. vol. 6. San Diego: Academic Press; 2008. p. 1-32.

89. Rice FL, Fundin BT, Arvidsson J, Aldskogius H, Johansson O. Comprehensive immunofluorescence and lectin binding analysis of vibrissal follicle sinus complex innervation in the mystacial pad of the rat. J Comp Neurol. 1997; 385:149–184. [PubMed: 9268122]

90. Richardson JD, Vasko MR. Cellular mechanisms of neurogenic inflammation. J Pharmacol Exp Ther. 2002; 302:839–845. [PubMed: 12183638]

91. Rodriguez Parkitna J, Korostynski M, Kaminska-Chowaniec D, Obara I, Mika J, Przewlocka B, Przewlocki R. Comparison of gene expression profiles in neuropathic and inflammatory pain. J Physiol Pharmacol. 2006; 57:401–414. [PubMed: 17033093]

92. Roosterman D, Goerge T, Schneider SW, Bunnett NW, Steinhoff M. Neuronal control of skin function: the skin as a neuroimmunoendocrine organ. Physiol Rev. 2006; 86:1309–1379. [PubMed: 17015491]

93. Sams A, Yenidunya A, Engberg J, Jansen-Olesen I. Equipotent in vitro actions of alpha- and beta-CGRP on guinea pig basilar artery are likely to be mediated via CRLR derived CGRP receptors. Regul Pept. 1999; 85:67–75. [PubMed: 10651059]

94. Sauer SK, Reeh PW, Bove GM. Noxious heat-induced CGRP release from rat sciatic nerve axons in vitro. Eur J Neurosci. 2001; 14:1203–1208. [PubMed: 11703449]

95. Schmitz JE, Simon MA, Kuroda MJ, Lifton MA, Ollert MW, Vogel CW, Racz P, Tenner-Racz K, Scallon BJ, Dalesandro M, Ghrayeb J, Rieber EP, Sasseville VG, Reimann KA. A nonhuman primate model for the selective elimination of CD8+ lymphocytes using a mouse-human chimeric monoclonal antibody. Am J Pathol. 1999; 154:1923–1932. [PubMed: 10362819]

96. Scholzen T, Armstrong CA, Bunnett NW, Luger TA, Olerud JE, Ansel JC. Neuropeptides in the skin: interactions between the neuroendocrine and the skin immune systems. Exp Dermatol. 1998; 7:81–96. [PubMed: 9583747]

97. Schutz B, Mauer D, Salmon AM, Changeux JP, Zimmer A. Analysis of the cellular expression pattern of beta-CGRP in alpha-CGRP-deficient mice. J Comp Neurol. 2004; 476:32–43. [PubMed: 15236465]

98. Schwenger N, Dux M, de Col R, Carr R, Messlinger K. Interaction of calcitonin gene-related peptide, nitric oxide and histamine release in neurogenic blood flow and afferent activation in the rat cranial dura mater. Cephalalgia. 2007; 27:481–491. [PubMed: 17441973]

99. Seiffert K, Granstein RD. Neuroendocrine regulation of skin dendritic cells. Ann N Y Acad Sci. 2006; 1088:195–206. [PubMed: 17192566]

100. Seike M, Ikeda M, Morimoto A, Matsumoto M, Kodama H. Increased synthesis of calcitonin gene-related peptide stimulates keratinocyte proliferation in murine UVB-irradiated skin. J Dermatol Sci. 2002; 28:135–143. [PubMed: 11858952]

101. Slominski A, Wortsman J. Neuroendocrinology of the skin. Endocr Rev. 2000; 21:457–487. [PubMed: 11041445]

102. Slominski A, Wortsman J, Tobin DJ. The cutaneous serotoninergic/melatoninergic system: securing a place under the sun. FASEB J. 2005; 19:176–194. [PubMed: 15677341]

103. Springer J, Geppetti P, Fischer A, Groneberg DA. Calcitonin gene-related peptide as inflammatory mediator. Pulm Pharmacol Ther. 2003; 16:121–130. [PubMed: 12749828]

104. Takahashi K, Nakanishi S, Imamura S. Direct effects of cutaneous neuropeptides on adenylyl cyclase activity and proliferation in a keratinocyte cell line: stimulation of cyclic AMP formation by CGRP and VIP/PHM, and inhibition by NPY through G protein-coupled receptors. J Invest Dermatol. 1993; 101:646–651. [PubMed: 8228323]

105. Tominaga M, Caterina MJ, Malmberg AB, Rosen TA, Gilbert H, Skinner K, Raumann BE, Basbaum AI, Julius D. The cloned capsaicin receptor integrates multiple pain-producing stimuli. Neuron. 1998; 21:531–543. [PubMed: 9768840]

106. Toyoda M, Luo Y, Makino T, Matsui C, Morohashi M. Calcitonin gene-related peptide upregulates melanogenesis and enhances melanocyte dendricity via induction of keratinocyte-derived melanotrophic factors. J Investig Dermatol Symp Proc. 1999; 4:116–125.

107. Tsukiji J, Sango K, Udaka N, Kageyama H, Ito T, Saito H, Horie H, Inoue S, Kitamura H, Hagiwara E, Ikeda H, Okubo T, Ishigatsubo Y. Long-term induction of beta-CGRP mRNA in rat lungs by allergic inflammation. Life Sci. 2004; 76:163–177. [PubMed: 15519362]

108. Ugawa S, Ueda T, Yamamura H, Shimada S. In situ hybridization evidence for the coexistence of ASIC and TRPV1 within rat single sensory neurons. Brain Res Mol Brain Res. 2005; 136:125–133. [PubMed: 15893596]

109. van Rossum D, Hanisch UK, Quirion R. Neuroanatomical localization, pharmacological characterization and functions of CGRP, related peptides and their receptors. Neurosci Biobehav Rev. 1997; 21:649–678. [PubMed: 9353797]

110. Williams K, Westmoreland S, Greco J, Ratai E, Lentz M, Kim WK, Fuller RA, Kim JP, Autissier P, Sehgal PK, Schinazi RF, Bischofberger N, Piatak M, Lifson JD, Masliah E, Gonzalez RG. Magnetic resonance spectroscopy reveals that activated monocytes contribute to neuronal injury in SIV neuroAIDS. J Clin Invest. 2005; 115:2534–2545. [PubMed: 16110325]

111. Wimalawansa SJ. Calcitonin gene-related peptide and its receptors: molecular genetics, physiology, pathophysiology, and therapeutic potentials. Endocr Rev. 1996; 17:533–585. [PubMed: 8897024]

112. Wimalawansa SJ, Morris HR, MacIntyre I. Both alpha- and beta-calcitonin gene-related peptides are present in plasma, cerebrospinal fluid and spinal cord in man. J Mol Endocrinol. 1989; 3:247–252. [PubMed: 2590386]

113. Yohn JJ, Morelli JG, Walchak SJ, Rundell KB, Norris DA, Zamora MR. Cultured human keratinocytes synthesize and secrete endothelin-1. J Invest Dermatol. 1993; 100:23–26. [PubMed: 8423387]

114. Yu XJ, Li CY, Xu YH, Chen LM, Zhou CL. Calcitonin gene-related peptide increases proliferation of human HaCaT keratinocytes by activation of MAP kinases. Cell Biol Int. 2009; 33:1144–1148. [PubMed: 19651223]

115. Yuspa SH, Kilkenny AE, Steinert PM, Roop DR. Expression of murine epidermal differentiation markers is tightly regulated by restricted extracellular calcium concentrations in vitro. J Cell Biol. 1989; 109:1207–1217. [PubMed: 2475508]

116. Zegarska B, Lelinska A, Tyrakowski T. Clinical and experimental aspects of cutaneous neurogenic inflammation. Pharmacol Rep. 2006; 58:13–21. [PubMed: 16531625]

117. Zhao P, Barr TP, Hou Q, Dib-Hajj SD, Black JA, Albrecht PJ, Petersen K, Eisenberg E, Wymer JP, Rice FL, Waxman SG. Voltage-gated sodium channel expression in rat and human epidermal keratinocytes: evidence for a role in pain. Pain. 2008; 139:90–105. [PubMed: 18442883]

118. Zimmermann M. Ethical guidelines for investigations of experimental pain in conscious animals. Pain. 1983; 16:109–110. [PubMed: 6877845]

119. Zylka MJ, Rice FL, Anderson DJ. Topographically distinct epidermal nociceptive circuits revealed by axonal tracers targeted to Mrgprd. Neuron. 2005; 45:17–25. [PubMed: 15629699]
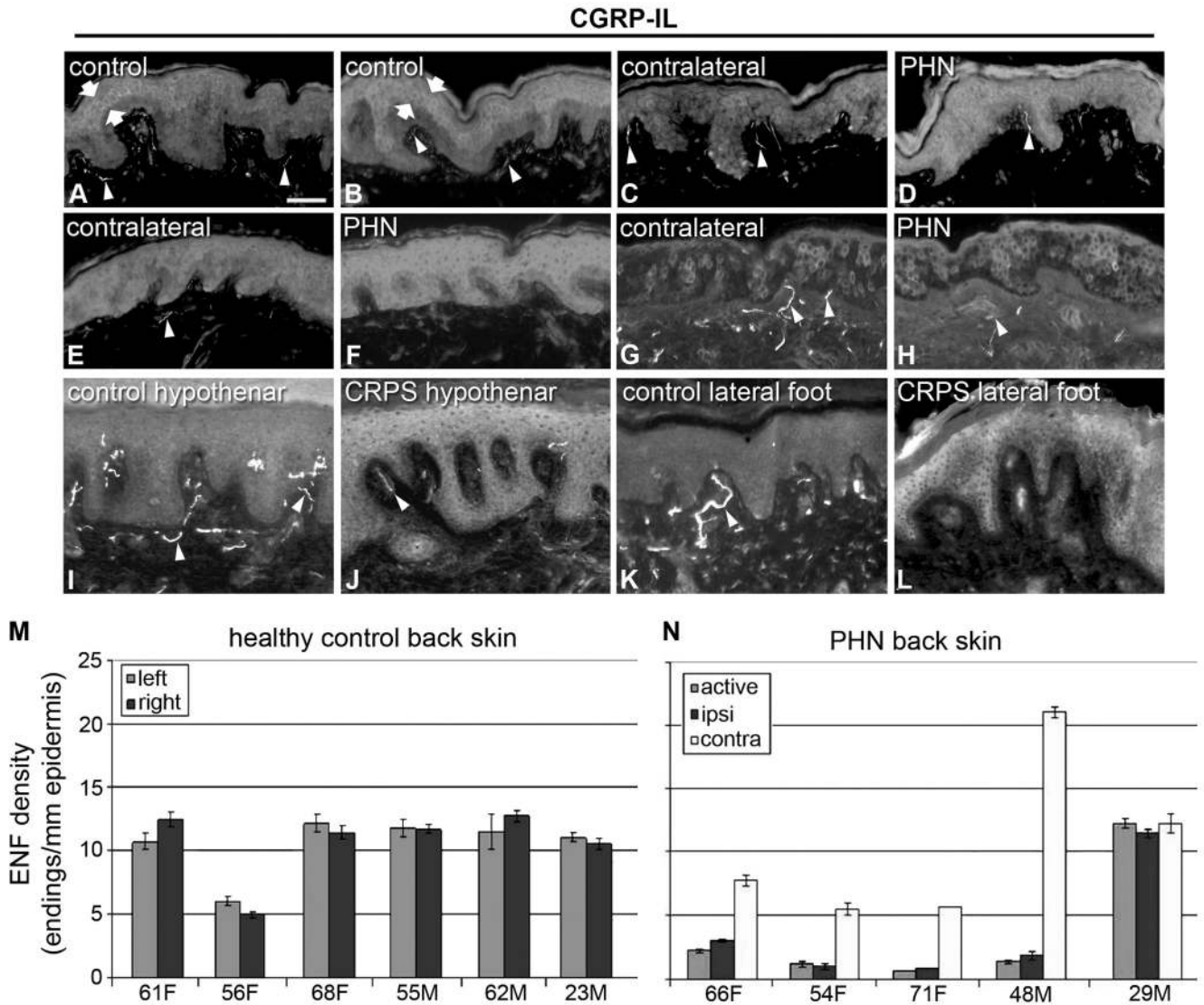
CGRP-IL

Figure 1. Increased CGRP expression in keratinocytes from human painful conditions
A–H) Images from sections of thoracic back skin biopsies processed with polyclonal anti-human CGRPα (A–F) captured at the same camera settings, and monoclonal anti-human CGRPα (G,H) captured at a higher camera sensitivity. Keratinocyte labeling is shown between arrows. Innervation labeling is shown with arrowheads. A, B) Examples of the variations in CGRP-IL expression among keratinocytes as shown in images from the left and right side respectively in a control subject (23-year old male) that had the *most* intense expression encountered among six control subjects. The CGRP-IL is heterogenous among keratinocytes mostly located in the middle third of the epidermis. C, D) Examples of CGRP-IL labeling among keratinocytes in a subject (29-year-old male) that had the *least* difference in labeling intensity between the PHN afflicted skin (D, VAS = 6.5) and the nonpainful unafflicted mirror-image contralateral skin (C). E, F) Examples of CGRP-IL labeling in a subject (48 year-old male, VAS = 5.0) that was representative of most of the PHN afflicted skin (F) and nonpainful unafflicted mirror-image contralateral skin (E). As revealed with the polyclonal antibody, nonpainful contralateral skin consistently had less intense and more heterogenous labeling of keratinocytes, whereas PHN skin had more intense and more

homogenous labeling. In both the afflicted and unafflicted skin of the PHN subjects, CGRP-IL was expressed among keratinocytes spanning most of the thickness of the epidermis. In the PHN skin, the stratum basalis was usually less intensely labeled than the more superficial strata. CGRP positive innervation (arrowheads) appears to be less in PHN skin than in contralateral skin or control skin. E–H) Comparison of polyclonal (E, F) versus monoclonal (G, H) CGRP-IL in sections from the same biopsies from the same subject. Monoclonal CGRP-IL of keratinocytes was far less intense and more heterogenous than polyclonal labeling, but was still more intense and widespread among keratinocytes in the PHN (H) versus the contralateral skin (G). Because of the higher camera sensitivity setting, innervation labeled with the monoclonal antibody appears more intense than that with the polyclonal antibody (arrowheads). I–L) Examples of polyclonal CGRP-IL among keratinocytes from the hypothenar (I, J) and lateral foot (K, L) of control subjects (I, K) and subjects with severe CRPS type 1 (J, L). CGRP-IL among keratinocytes has a very low intensity in control skin and a moderate to high intensity among CRPS skin. In the CRPS skin, there are fewer and more weakly CGRP-IL detectable axons and endings in the upper dermis and epidermis than in control skin (arrowheads). Scale bar = 65µm in A–H, 50µm in I–L. M, N) Similar to other published reports, PGP-IL of epidermal endings from healthy controls (M) and the PHN patient cohort (N) reveals decreased epidermal nerve fiber density among the active PHN and ipsilateral sites compared with a mirror-image contralateral site, in 4 of the 5 PHN subjects, whereas healthy controls showed no lateral differences.
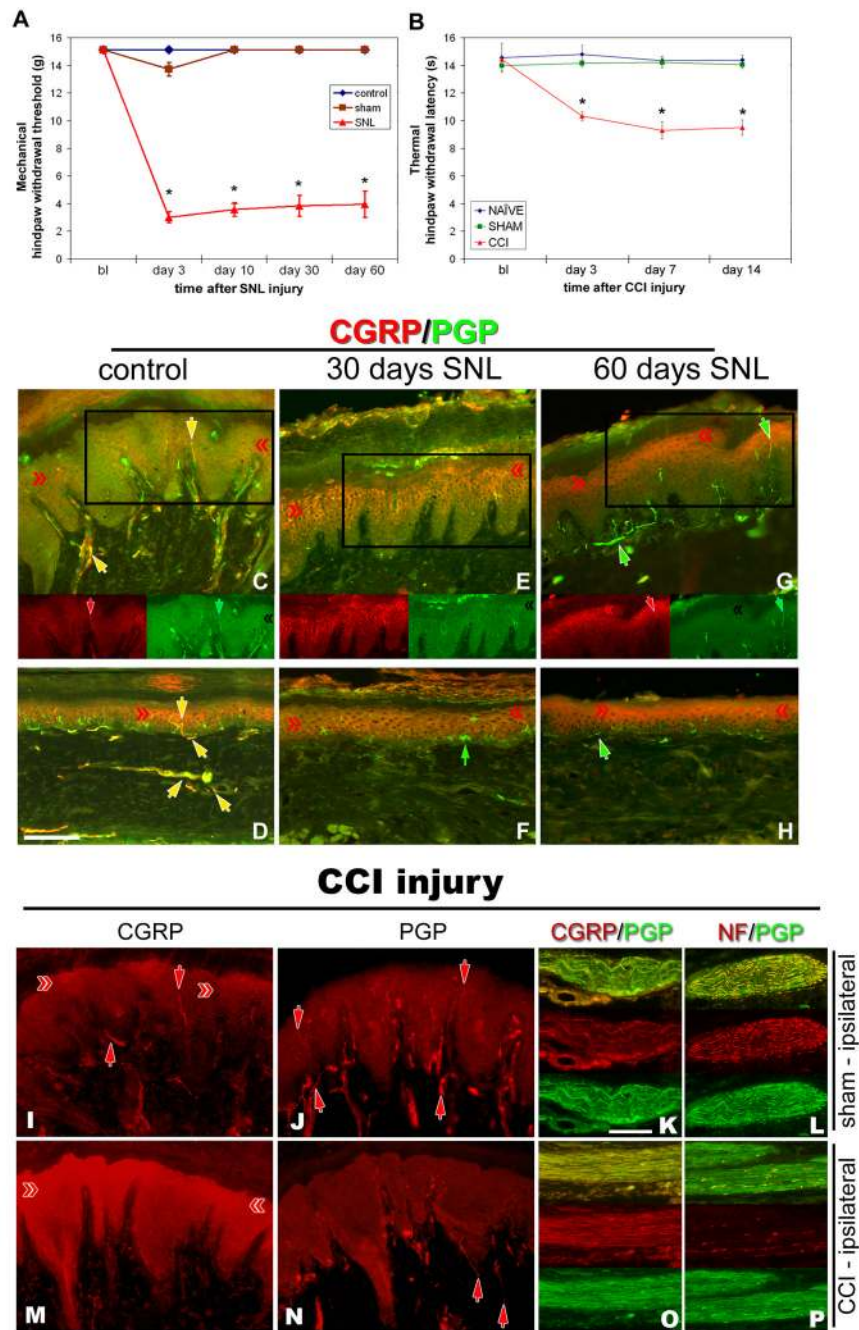
Figure 2. Nerve injury models of neuropathic pain increase CGRP expression in epidermal keratinocytes

Nocicieptive behaviors were induced in rats by SNL (A) or sciatic CCI (B), and following SNL (C–H) or sciatic CCI (I–P), CGRP-IL increases are evident in hindpaw epidermal keratinocytes (red chevrons), with a reduction in peptidergic cutaneous innervation compared to control skin (yellow and red arrows). A) Graph depicting the extent of chronic neuropathic mechanical allodynia (Von Frey filaments) following SNL, demonstrating persistence out to at least 60 days, at a time corresponding to increased CGRP-IL among the keratinocytes. B) Graph depicting the extent of chronic neuropathic thermal hyperalgesia (Hargreaves test) following CCI, demonstrating persistence out to 14 days, at a time

corresponding to increased CGRP-IL among the keratinocytes. C–P) Representative photomicrographs of single or double (merged) label immunocytochemistry for calcitonin-gene related peptide (CGRP, red) or 200kD neurofilament (NF, red) and protein gene product 9.5 (PGP, green). Previous studies have shown that anti-PGP labels all types of innervation, whereas 200kD NF immunolabeling is normally expressed in, and limited to, thick caliber Aβ fibers and thin caliber Aδ fibers. C fibers normally lack NF-IL. CGRP-IL is normally observed in subsets of C and Aδ fibers. C,D) Control, unoperated rats show intense CGRP-IL of axonal innervation (PGP positive, double labeled structures) among the epidermal endings, dermal vasculature endings, and subepidermal and dermal fibers (yellow arrows). Epidermal keratinocyte CGRP-IL (red chevrons) is heterogeneous and moderate among the volar pad crown (C) and flat (D) glabrous hindpaw skin, and remains largely suprabasal. E,F) By 30 days following SNL, a near complete loss of neural innervation is observed (i.e., no PGP nerve labeling; small green arrow in F shows a Langerhans cell, which are known to express PGP), while epidermal keratinocyte CGRP expression appears more extensive throughout suprabasal keratinocytes among the pad crown (E) and flat (F) glabrous hindpaw skin (red chevrons). G, H) By 60 days following SNL, neural innervation has begun to return (PGP axons, green arrows), but largely without a CGRP contingent, whereas the epidermal keratinocyte expression of CGRP remains elevated among pad crown (G) and flat (H) glabrous hindpaw skin (red chevrons). I–L) Sham-operated, non-CCI rats have epidermal keratinocyte expression of CGRP that is heterogeneous and weak among the volar pad crown (I, red chevrons), with intense CGRP immunolabeling of a subset of PGP-positive axonal innervation (I, red arrows; J, PGP positive, red arrows) among the epidermal endings (downward red arrows), and upper dermal fibers (upward red arrows), and within dermal nerves (K, red panel). NF content within the dermal nerves was extensively distributed among mostly the larger caliber axons and some small caliber axons (L, red panel). M–P) CCI rats showed dramatically elevated expression of CGRP among the suprabasal keratinocytes (M, red chevrons), coincident with depleted CGRP-IL epidermal endings and dermal nerve fibers, among an overall depleted innervation (N, PGP positive, red arrows). Interestingly, CGRP content appears to be increased within deep dermal nerves (O, red panel), but was mostly distributed among vacuolated cells affiliated with the larger caliber axons. NF-IL is severely depleted among the large caliber axons within the deep nerves, indicating that these axons may be deteriorating and that the vacuolated cells may be reactive Schwann cells (P, red panel). Magnification bar (D) =50µm for C–H, and I,J,M,N; (K)=25µm for K,L,O,P.
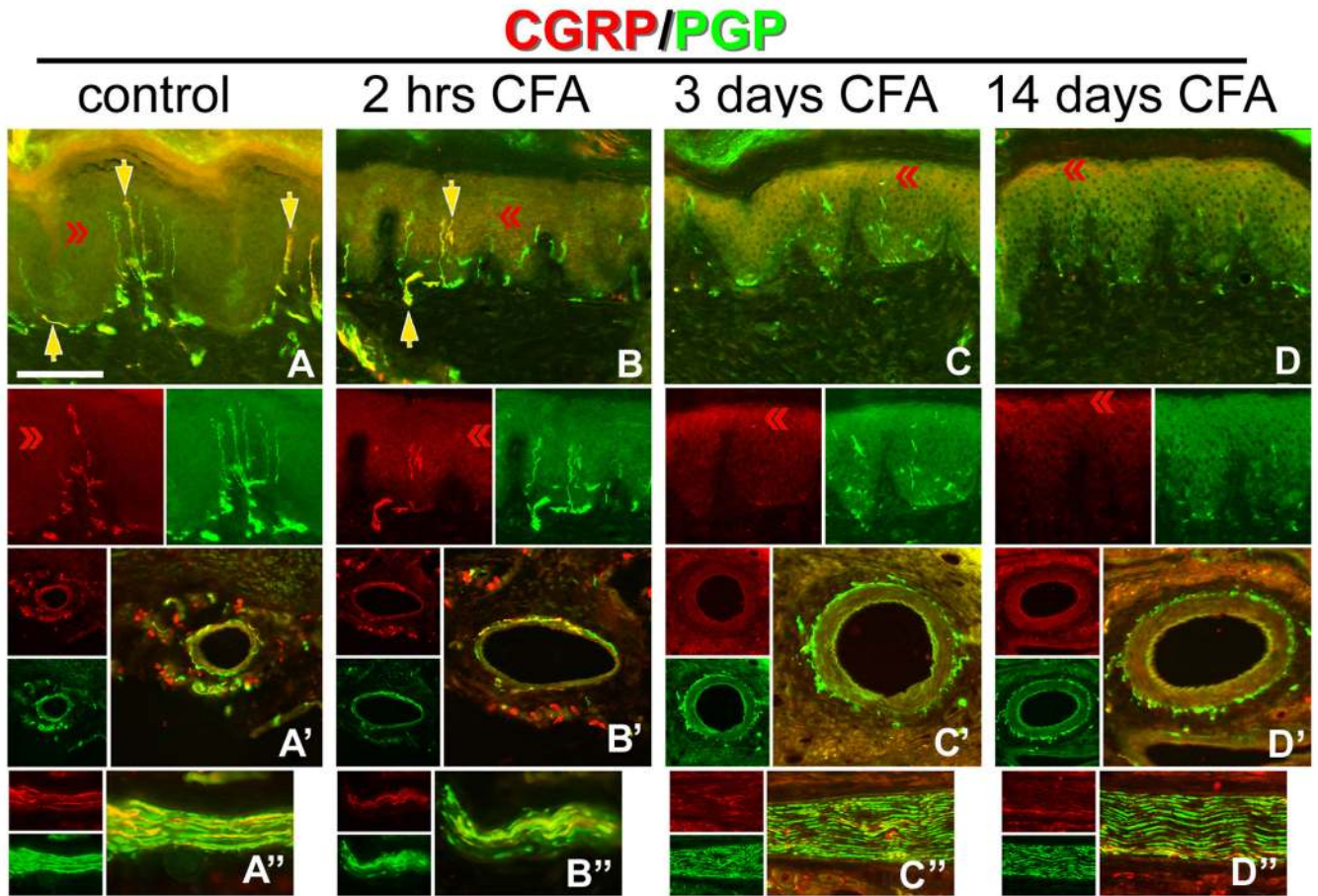
Figure 3. Hindpaw inflammation increases CGRP expression in epidermal keratinocytes
A–D) CFA hindpaw injection time course, depicting in each vertical panel, representative double label (CGRP/PGP) results from glabrous pad crown (A–D), dermal vasculature ('), and dermal nerve (''), with each separate channel split below or to the left of the double label image. A) Control uninjected rats depicting CGRP-IL of a subset of innervation (PGP-IL, green) among the epidermal endings and subepidermal plexus (yellow arrows). The separate channels are split below the double labeled images. Epidermal keratinocyte CGRP-IL (red chevrons) appeared heterogeneous and weak among the volar pad crown. A') Neural innervation to dermal vasculature contained a mix of CGRP-IL-positive and CGRP-IL-negative axons among the tunica media and advential layers. A'') Dermal nerves contained a rich contingent of CGRP-IL axons. B) By 2 hrs after CFA injection, increased CGRP expression is apparent among epidermal keratinocytes, with little change among the innervation of the epidermis, subepidermal plexus, dermal vasculature (B'), or in the composition of dermal nerves (B''). C) By 3 days after CFA injection, epidermal CGRP expression is increased among suprabasal keratinocytes, while neural innervation appears depleted (i.e., lack of CGRP or PGP axon staining) from the epidermis and subepidermal plexus. C') Interestingly, among the dermal vasculature, a dramatic loss of CGRP immunopositive medial and adventitial innervation is observed, although PGP immunopositive axons are still present. Dermal nerves appear distraught with ragged PGP labeling and limited CGRP axons present (C''). D) By 14 days following CFA, epidermal CGRP expression remains elevated among the most suprabasal keratinocytes, and immunopositive axons are absent from the epidermis or subepidermal plexus. D') Dermal vasculature appeared without CGRP immunopositive innervation among the medial and

adventitial layers, although PGP immunopositive axons were still present, and dermal nerves remained distraught in appearance with limited CGRP axons (D"). Magnification bar (A) =50µm for A–D, and =25µm for (') and (''). Anti-CGRP (guinea pig polyclonal, 1:800; Peninsula Labs, San Carlos, CA) and anti-PGP (rabbit polyclonal, 1:1000; UltraClone, Wellow, UK) were used.
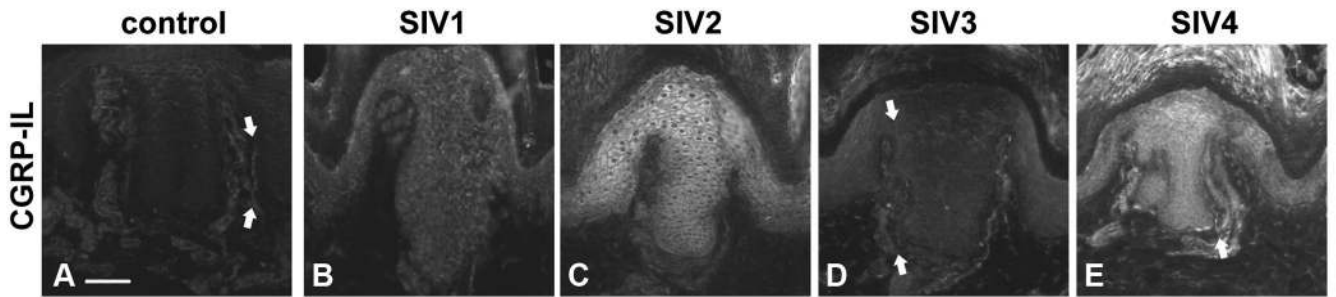
Figure 4. SIV infection in rhesus macaques results in an increase of CGRP-IL in epidermal keratinocytes

A–E) CGRP-IL is increased among palmar glabrous skin keratinocytes from SIV-infected animals compared with control epidermis. A) Control monkey epidermal primary ridge depicting CGRP-IL among fine delicate innervation of the epidermis, and upper dermal compartments (downward and upward arrows, respectively). B–E) Compared with the control monkey, all monkeys infected with SIV had increased CGRP-IR, although the intensity varied between monkeys. B) As seen in an aged monkey with AIDS and severe SIV encephalitis (SIVE), moderate CGRP-IL is detected among the epidermal keratinocytes. C) This young adult monkey had no AIDS defining illness, but did show abundant systemic viral replication and had severe colitis at the time of sacrifice. Dramatic increases in CGRP-IL of keratinocytes can be seen. D) This represents a similarly young adult monkey with SIV infection, with the most subtle increase in epidermal keratinocyte CGRP-IL observed. In this animal, CGRP-IL among keratinocytes was only slightly higher compared with the control or other SIV animals, and CGRP-IL innervation was observed (arrows). E) This represents another young adult SIV infected animal, demonstrating robust CGRP-IL of epidermal keratinocytes, and CGRP-IL among upper dermal nerves (arrow). Magnification bar (A) =50µm for A–E. Anti-CGRP (guinea pig polyclonal, 1:800; Peninsula Labs, San Carlos, CA) was used.
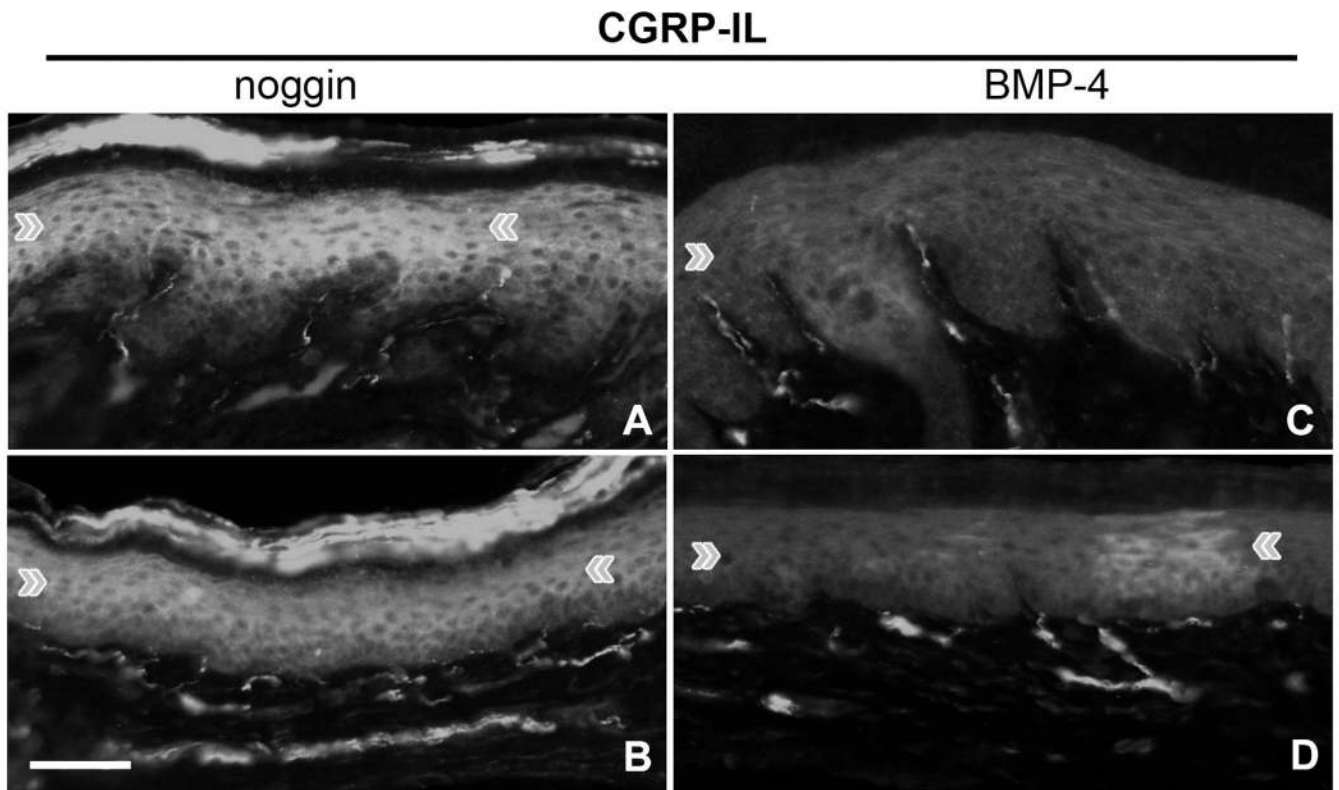
Figure 5. Epidermal keratinocyte CGRP-IL is effected by the noggin/BMP4 system
Utilizing transgenic mice which over-produce noggin or BMP4 driven off of the K14 promoter, hindpaw skin was removed and immunolabeled for CGRP. A,B) Noggin over-expression results in intense CGRP-IL in keratinocytes among the volar pad crown (A) and flat (B) glabrous hindpaw skin, appearing more extensive throughout suprabasal keratinocytes. C,D) BMP4 over-expression results in little CGRP-IL in keratinocytes among the volar pad crown (E) and flat (F) glabrous hindpaw skin. The BMP4 keratinocyte expression appeared heterogeneous and similar to that observed in control rats (see Fig. 2C, I). Note that CGRP immunolabeling on nerve fibers was present in the skin of both noggin and BMP4 over-expressing mice, although a prior study detected differences among subtypes of CGRP-positive fibers. Magnification bar =50µm. Anti-CGRP (rabbit polyclonal, 1:1000; Chemicon Inc, Temecula, CA) was used.
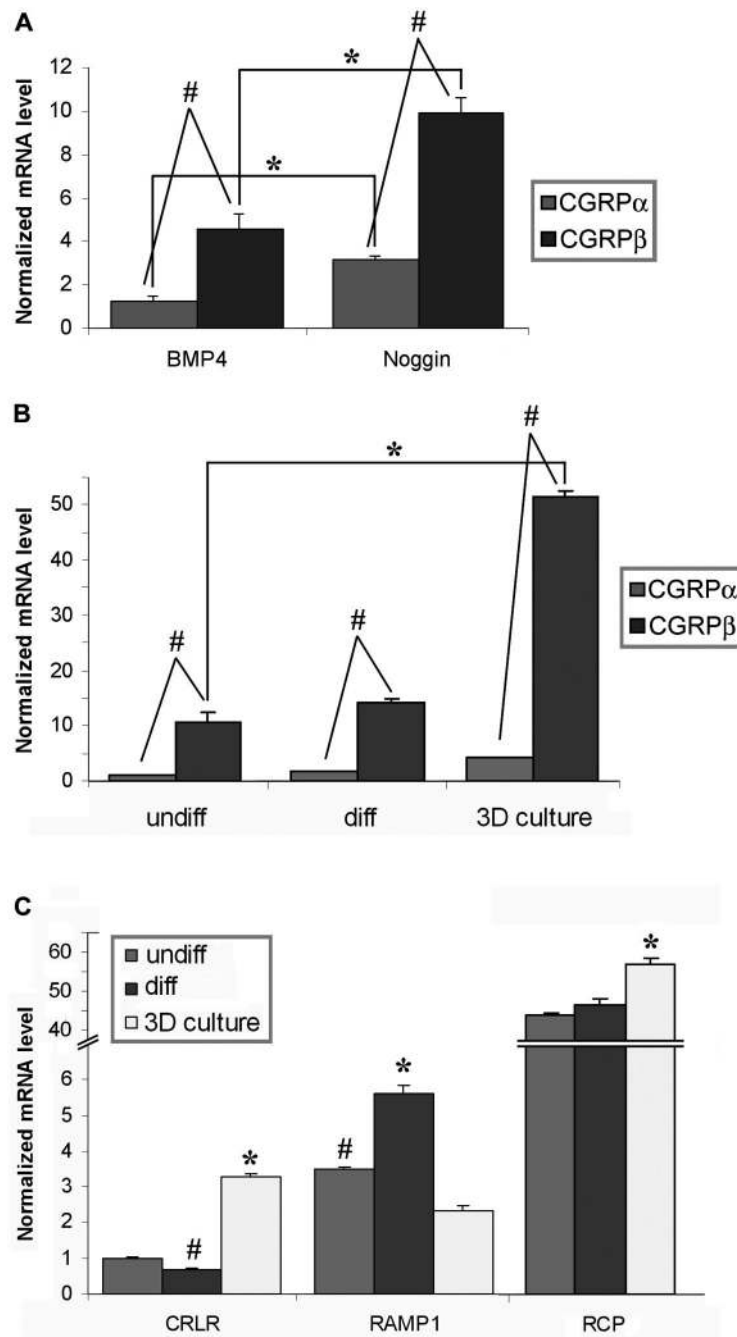
Figure 6. CGRP mRNA expression in transgenic mouse epidermal keratinocytes *in vivo*, and normal human keratinocytes *in vitro*

Real time quantitative PCR was performed using primers specific to CGRPα, CGRPβ, BMP4, noggin, and members of the CGRP receptor complex, CRLR, RAMP1, and RCP. A–C) Data is presented as relative mRNA levels, normalized to the reference gene GAPDH. A) Epidermal glabrous skin compartments were obtained by laser capture microdissection from BMP4 or noggin over-expression transgenic mice. Total mRNA was obtained from a pool of 5–7 etched epidermis' per sample. Transgenic over-expression of noggin results in significantly greater expression of CGRPα and CGRPβ mRNA compared with the BMP4 over-expressing transgenic mice (*). As well, the CGRPβ isoform is expressed in

significantly greater amounts (~3.5-fold) than the CGRPα isoform among both lines of transgenic mice (#). B) Normal human epidermal keratinocytes (NHEK) were cultured with standard media (undiff), or calcium differentiated with 2M $CaCl_2$ (diff), and primary human keratinocytes were grown as a 3D raft culture at the air interface, allowing for stratification and formation of an oragnotypic psudoepidermis (3D raft). Keratinocyte differentiation significantly increases the production of both CGRP mRNA isoforms compared with undifferentiated NHEK cells (*). Importantly, under all three keratinocyte growth conditions, data demonstrates that the CGRPβ isoform is expressed in undifferentiated NHEK (10.4-fold increase), differentiated NHEK (8.0-fold increase), and 3D raft cultures (12.3 fold increase), to a significantly greater degree than the CGRPα isoform (#). C) Under all keratinocyte growth conditions, the complete receptor complex components specific for CGRP were detected. For A–C, * and # $p < 0.05$ by Student's t-test.
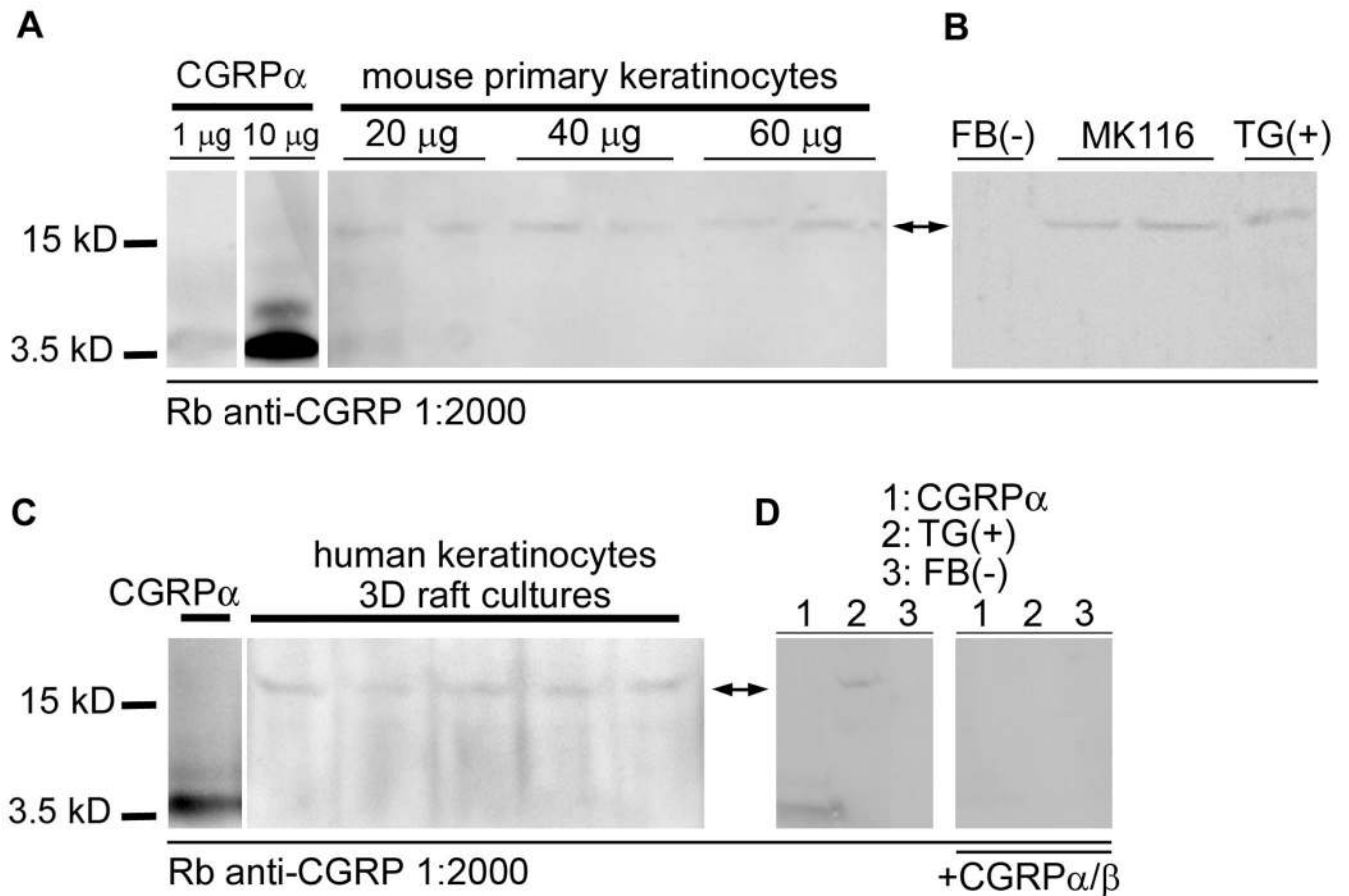
Figure 7. CGRP precursor protein is expressed in mouse and human keratinocytes using western blot

Total protein was isolated from primary and immortalized mouse keratinocytes (MK116), three-dimensional cultured human epidermal keratinocytes (3D raft cultures), cultured mouse fibroblasts (FB), and mouse trigeminal ganglia (TG). Western blot analysis was performed to determine CGRP protein content. A) Duplicate protein samples from primary mouse keratinocytes were loaded at 20, 40, and 60 µg/lane, along with CGRPα positive control lanes, separated, transferred to PDVF nylon membranes and probed with anti-CGRP (Rb polyclonal, 1:2000; Chemicon Inc, Temecula, CA). A low level detectable band was observed from all samples at the predicted weight of CGRP precursor protein (16kDa; arrows). The positive control CGRPα was detected at the processed size (~3.7kD), however, among the *in vitro* cultures, no mature peptide was detectable. B) Total protein samples from mouse fibroblasts (FB, as negative control), immortalized mouse keratinocytes (MK116), and mouse trigeminal ganglia (TG, as positive control) were loaded (20 µg/lane), separated, transferred to PDVF nylon membranes and probed with anti-CGRP (Rb polyclonal, 1:2000; Chemicon Inc, Temecula, CA). A detectable band corresponding to the predicted molecular weight of the CGRP precursor protein (16kD; arrows) was observed in the keratinocyte and trigeminal ganglia lanes, but was not detectable in the fibroblast lane. C) Total protein samples from organotypic human keratinocytes (3D raft cultures) were loaded, along with CGRPα positive control, separated, transferred to PDVF nylon membranes and probed with anti-CGRP (Rb polyclonal, 1:2000; Chemicon Inc, Temecula, CA). A detectable band corresponding to the predicted molecular weight of the CGRP precursor protein (16kD; arrows) was observed in all lanes. D) Total protein samples from

mouse trigeminal ganglia (TG, positive control) and mouse fibroblasts (FB, negative control) were loaded (20 µg/lane), along with CGRPα (1µg) positive control, in duplicate, separated, transferred to PDVF nylon membranes, and the membrane then separated. One half of the membrane (left) was then probed with anti-CGRP (Rb polyclonal, 1:2000; Chemicon Inc, Temecula, CA), while the other half (right) was probed with pre-adsorbed anti-CGRP antibody. Mature CGRP (~3.7kD) and CGRP precursor protein (16kD; arrows) bands were detected on the left membrane, and no bands were detectible on the right membrane after specific primary antibody pre-adsorption.

NIH-PA Author Manuscript   NIH-PA Author Manuscript   NIH-PA Author Manuscript

Table 1

Human PHN and Control Subject Demographics

age	gender	derm	Dx	HTN	chol	hypothy	VAS	BPI-S	BPI-I
66	female	T8	PHN	no	no	yes	3.0	3.8	2.3
54	female	L1	PHN	yes	no	no	4.8	3.3	5.6
71	female	C5	PHN	no	no	no	3.5	3.5	1.7
48	male	T6	PHN	no	yes	no	5.0	2.8	1.4
29	male	C4	PHN	no	yes	no	6.5	5.0	5.0
61	female	T8	HC	yes	yes	yes			
56	female	L1	HC	no	no	no			
68	female	C5	HC	no	no	no		n/a	
55	male	T6	HC	no	no	no			
62	male	C5	HC	no	no	no			
23	male	C5	HC	no	no	no			

Table 2

SIV Monkey Demographics

animal	gender	age	diagnosis comments
CNTL	male	~7 yr	control, healthy uninfected
SIV1	male	12 yr, 6 mo	AIDS with severe SIVE
SIV2	male	3 yr, 10 mo	no AIDS defining illness 42 days after infection; sacrificed due to chronic colitis
SIV3	male	3 yr, 8 mo	sacrificed due to AIDS
SIV4	male	3 yr 3 mo	sacrificed due to AIDS

Table 3

Antibodies Utilized for these studies

Antibody	Production Antigen	Species	Source	Type	Use	Dilution
anti-CGRP	synthetic rat CGRPα	Rb polyclonal	Millipore/Chemicon	serum	IHC, WB	1:1000, 1:800
anti-CGRP	synthetic Hu CGRPα	Gp polyclonal	Peninsula	serum	IHC	1:800
anti-CGRP	synthetic Hu CGRPα	Ms monoclonal	Cayman	AP	IHC, EIA	1:1000, N/A
anti-PGP	purifed Hu brain PGP	Rb polyclonal	UltraClone	serum	IHC	1:1000
anti-NF(200)	purified bovine NF	Rb polyclonal	Millipore	serum	IHC	1:800